Ph.D. thesis

The effect of tropomyosin and heavy meromyosin on the flexibility of formin-nucleated actin filaments

ZOLTÁN UJFALUSI

Supervisor:
Prof. Dr. Miklós Nyitrai
Director of the Department of Biophysics

University of Pécs
Medical School
Department of Biophysics

Pécs, 2012

Interdisciplinary Medical Sciences Doctoral School D93

Head of Doctoral School: Prof. Dr. Balázs Sümegi

Program: B-130: Investigating functional protein dynamics using biophysical methods

Program leader: Prof. Dr. Miklós Nyitrai

Supervisor: Prof. Dr. Miklós Nyitrai

"The important thing is not to stop questioning. Curiosity has its own reason for existing."

Albert Einstein

Acknowledgements

I would like to express my sincere thanks to my supervisor, Professor Dr. Miklós Nyitrai for the perfect way of guidance. His support, his way of thinking, his immense knowledge and encouragement have been inspiring for me all the time.

I wish to express my sincere gratitude to Professor Dr. Béla Somogyi for receiving me in the Department of Biophysics and providing a friendly atmosphere here.

I am deeply grateful to Dr. Beáta Bugyi and Dr. Gábor Hild for their kind help and detailed and constructive advices.

I warmly thank Dr. Gábor Papp, Dr. József Orbán and Dr. László Grama for their excellent advices and friendly help throughout my research.

My sincere thanks to Szilvia Barkó and Veronika Kollár for their constructive criticism and valuable advices regarding my work and for the very friendly atmosphere they provide.

I also wish to thank Jánosné Brunner and Erzsébet Garajszkiné Papp for their essential assistance in the lab.

Furthermore, I wish to thank all of my colleagues at the Department of Biophysics for their kind support and daily help.

My forever lasting gratitude is due to my Mother, Grandmother and Brother, for their loving and inexhaustible support from the day of my birth.

Last but not least I owe my loving thanks to my wife Kinga and to my son Benjámin. They gave a new meaning to my life and without their love, encouragement and understanding it would have been impossible to finish my thesis.

Table of contents

1 General introduction

1.1 Actin

Actin plays indispensable roles in several processes in eukaryotic cells [1]. The dynamic actin network is essential for the determination and regulation of cell shape [2], polarity, cell division and the transport processes within eukaryotic cells [1, 3-9]. Formation of the actin structures requires the assembly of actin filaments, which is limited by the thermodynamically unfavourable nucleation [1, 10]. The concentration of free actin monomers (globular or G-actin) in the cytoplasm is very low (approx. 0.5 µM) and actin dimers (nuclei) are unstable [11]. Several prokaryotic proteins have structural similarities to eukaryotic actin and assemble into filaments, suggesting that they represent an ancestor of the actin cytoskeleton. These bacterial factors are murein formation cluster E B (MreB) [12, 13] and partitioning M (ParM) [14, 15].

Figure 1 – First photo ever made of an actin filament by electron microscope [16].

Actin was discovered by a then young biochemist, Brunó Straub, in the laboratory of Albert Szent-Györgyi in 1942 [17]. By that time Szent-Györgyi had already extracted low viscosity myosin (myosin A) from rabbit skeletal muscle with 0.6 M KCl solution in cold room. By letting the muscle soak in 0.6 M KCl solution, he obtained a very viscous myosin solution (myosin B). Straub thought that the difference between myosin A and myosin B is due to the presence of a new protein, which makes the product of the extract viscous. He extracted myosin A from muscle and left the

remainder in cold room overnight. The muscle leftover was washed with distilled water to get rid of the remaining KCl and cytoplasmic proteins and finally it was dried using acetone. The protein which can be extracted from this acetone-dried muscle powder forms a very viscous complex with myosin A, which is similar to myosin B. "It activated myosin" – he said and named the protein actin [18]. Straub found out that they can get low viscosity actin solution (monomer form, G-actin (*Fig. 2*)) by water-based extraction of the acetone powder. If we add salts to this solution its viscosity increases (filament form, F-actin, (*Fig. 1*)). Later Straub followed the polymerization of actin monomers with the help of a viscometer [19]. (Further information: http://actin.aok.pte.hu/archives/)

In 1950 Feuer and Straub observed that each actin monomer binds ATP and during polymerization this ATP hydrolyses to ADP + P_i [20]. It was 40 years later that Kabsch and his collaborators crystallized G-actin and determined its structure [21].

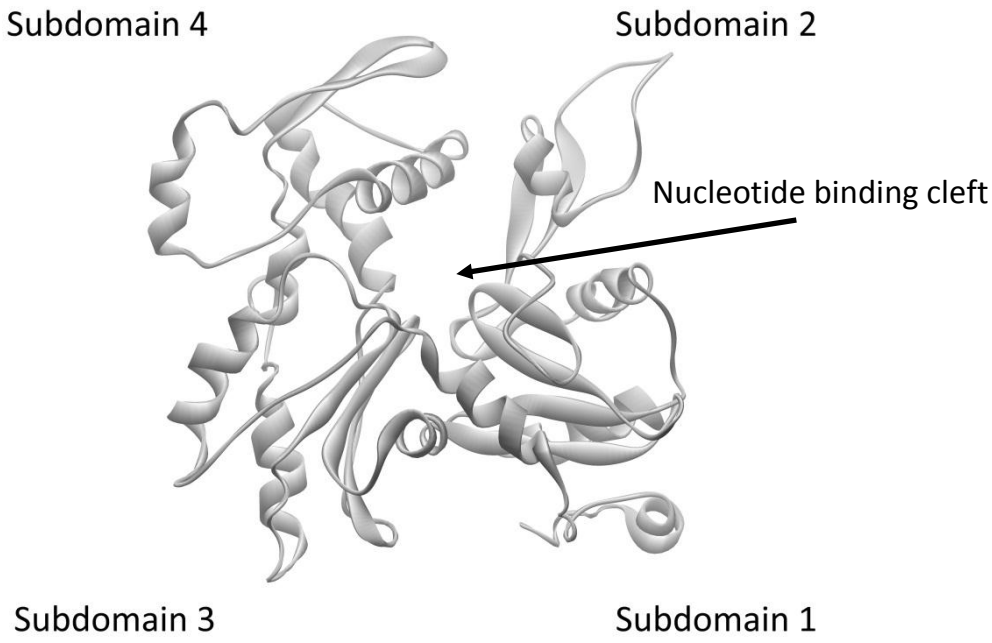

Figure 2 – The three dimensional structural model of the actin monomer (based on the pdb file *2ZWH*) indicating the four subdomains and the position of the nucleotide binding cleft.

Actin is the main component of the microfilament system, and it contributes 15 % to the total protein content of skeletal muscle. Its molecular weight is 42.3 kDa and it is composed of375 amino acids. In cells there are two forms of actin, the

monomer or globular (G-actin – *Fig. 2*) and the polymer or filament (F-actin – *Fig. 1*) forms. The filaments build up from monomers linked by non-covalent bonds. The structure of monomers can be divided into two domains, a smaller one and a larger one. The smaller domain contains subdomains 1 and 2, while the larger one contains subdomains 3 and 4 (*Fig. 2*). The cleft between the two domains contains the primary cation and nucleotide binding sites. Physiologically the bound divalent cation is Mg^{2+}, *in vitro* the cation is often Ca^{2+} to keep actin in monomeric form. The nucleotide binding site binds ATP, ADP.P_i or ADP.

The polymerization of the actin has three main phases. The first phase starts with the activation of monomers followed by the nucleation where two or three monomers bind to form a nucleus. This nucleation step is relatively slow because this process is thermodynamically unfavourable which also explains the instability of the dimers and trimers. The next phase of the polymerization is the diffusion-controlled elongation where monomers incorporate into the forming filament. In the last stage a dynamic equilibrium, the so-called 'treadmilling' is dominant. In this phase there is association and dissociation on both ends of a filament but the kinetics at each end are different. On one end of the filament monomers mainly incorporate to the filament (association) while on the other end they rather detach from the filament (dissociation), resulting in a filament length that does not change. One can say that actin filaments are polarized; they have a dynamically growing positive (barbed) end and a negative (pointed) end where the dissociation of the protomers is the main process. The protomers at the growing end bind ATP, while the protomers in the shortening end bind ADP because of the hydrolysis of ATP.

Actin is a highly conserved protein with many isoforms [22]. In this work we focused on the effects of proteins associated to the microfilament system of the cytoskeleton, however, the actin isoform we used in the experiments was extracted from rabbit skeletal muscle because of the highly efficient preparation. In skeletal muscle the smallest functional unit is the so-called sarcomere (*Fig. 3*), which is a molecular-scale structure, almost like a microscopic muscle. The mammalian sarcomere is ~ 2 µm in length and able to shorten to ~ 70 % of its original length during contraction. A sarcomere is defined as the segment between two neighbouring Z-lines (or Z-discs). Z-discs are surrounded by the I-band. Between two I-bands there is

the A-band. Within the A-band there is a brighter region called the H-zone (or H-band) and inside the H-zone there is a thin M-line (or M-band) [23]. A-bands and I-bands are named after anisotropic (dark bands in a polarizing light microscope due to their birefringent properties) and isotropic (bright bands in a polarizing light microscope because they have no birefringent properties), respectively. Actin filaments are the main components of the I-band extended into the A-band. Myosin filaments run throughout the A-band and are thought to overlap in the M-band [24]. Titin (also known as connectin) forms a continuous link from the M-band to the Z-line. Titin is the largest known protein. It acts as a molecular spring by restoring the length of the stretched sarcomere [23, 24]. The interaction between actin and myosin filaments in the A-band of the sarcomere is responsible for muscle contraction (*Fig. 3*). Several proteins important for the stability of the sarcomeric structure are found in the Z-disc as well as in the M-band of the sarcomere [24].

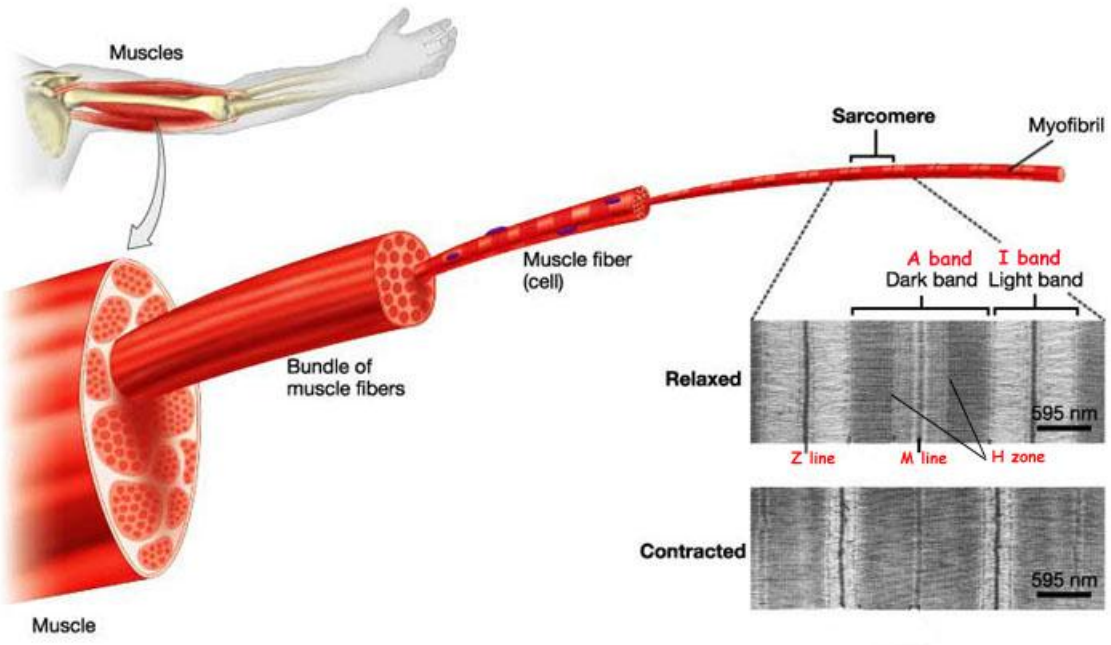

Figure 3 – From muscle to sarcomere [25]. A detailed schematic representation of skeletal muscle with a polarized light microscopy image in the right corner.

1.2 Formins as actin assembly factors

The dynamic assembly and turnover of actin networks determine cell polarity and facilitate membrane and organelle traffic, cell adhesion, chromosome segregation, cell migration and cell division [26, 27]. The *de novo* assembly of actin polymers requires active mechanisms, because there are lots of different factors in cells that counteract spontaneous polymer formation. These factors can be sequestering proteins, which help to maintain the pool of actin monomers (e.g. thymosins) and can be proteins that cap filament ends and sever or depolymerize them (e.g. ADF/Cofilin, capping proteins) *Fig. 4* [28]. To form new actin polymers cells deploy specialized proteins that can catalyse polymer nucleation and/or elongation, can protect growing polymer ends and can attach to the sides and/or ends of polymers to protect them against disassembly [29].

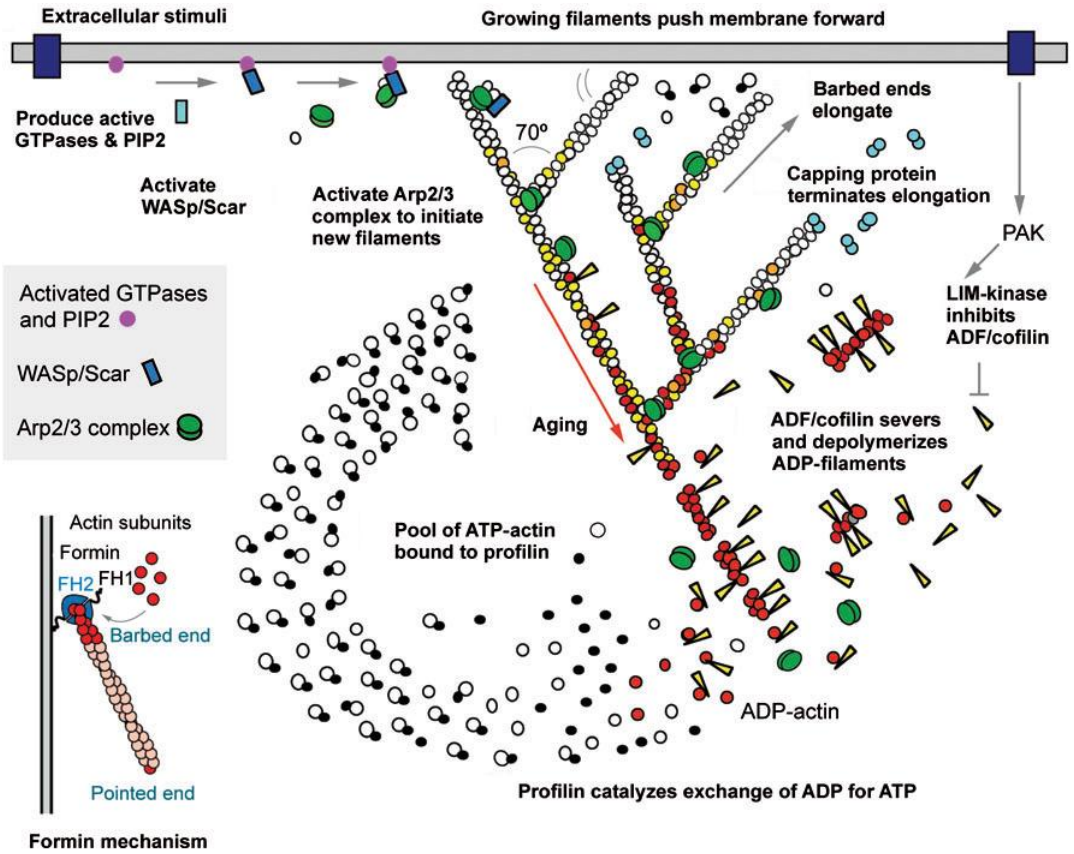

Figure 4 – An overview of the organization of the actin cytoskeleton at the leading edge of motile cells involving nucleating factors and other actin binding proteins [28]. One can see free barbed ends of filaments which grow until they are capped and formins that nucleate unbranched filaments and remain attached to the barbed ends as the filaments elongate. By contrast, the Arp2/3 complex binds to the side of a filament to nucleate a branch.

There are many actin-binding proteins identified so far. Those capping proteins that bind the barbed end of the filament inhibit the polymerization or depolymerisation of filamentous actin (e.g. CapZ protein [30]). If this inhibition allows no elongation and the capping protein binds actin with high affinity, we call it 'tight cap' or 'strong cap'; in the case of complete inhibition but low affinity we talk about 'weak cap'; when the inhibition of the elongation is just partial then the protein is a 'leaky cap' [31].

Members of the ADF/Cofilin family are able to sever actin filaments [32], while an other actin binding protein (ABP) can create new branches (Arp2/3 [33]). Formins represent a major group of actin nucleators along with the Arp2/3 complex [5, 34], Spire [35], Leiomodin [36] and Cordon-bleu [37].

Among the known nucleators the Arp2/3 complex is unique in its ability to nucleate filaments and organize them into branched networks. The Arp2/3 complex binds to a previously formed actin filament and initiates the assembly of a new one, joining the two at an ~ 70° Y-branch angle [38]. Spire was identified in *Drosophila melanogaster* as a factor required for egg and embryo development and it was shown to nucleate actin at a rate that is similar to that of the formin family of proteins – but lower than that of the activated Arp2/3 complex – and it remains associated with the slow-growing pointed end of the new filament [35]. Cordon-bleu (COBL) is an actin nucleator controlling neuronal morphology and development. It was identified in yeast two-hybrid assays as a factor that interacts with actin-binding protein 1 (ABP1) and syndapin, proteins that promote actin polymerization in brain extracts [37]. COBL seems to be a vertebrate-specific protein, and might bind profilin as well [39]. Leiomodin 2 (LMOD2), the recently discovered actin nucleating factor to be characterized [36], is expressed in skeletal and cardiac muscle and has homologues (LMOD1 and LMOD3) in smooth muscle and perhaps other tissues [40]. LMOD2 potently nucleates actin filaments *in vitro* without modifying elongation rates at either end [36].

Formins are conserved proteins in eukaryotes during the evolution. They can be identified by the presence of a highly conserved region, the so-called formin homology domain 2 (FH2). Varieties of formins act through the actin and microtubule systems and take part in meiosis, mitosis, cell movements, cell polarity, filopodia formation, embryonic development, sperm acrosome formation, endocytosis, etc.

[31]. The biochemical effect of formins on actin is strong, typically requiring only 5-200 nM formin for robust nucleation and/or elongation activity *in vitro* [29, 41]. These multi-domain proteins are present in many animal and plant species [4]. Numerous formin members are organized into families. Proteins of formin families play a very important role in the organization and rearrangement of the cytoskeleton. The first member of formin families was identified as a gene the mutation of which causes limb deformity. The effect of the deformity-causing mutation appears during morphogenesis in chicken and in rodents [42]. The mutation of hDia (a human homologue of mDia (mammalian Diaphanous-related formin)) is responsible for a type of deafness due to inadequate formation of the actin network within stereocilia of hair cells in the inner ear [43].

1.2.1 The structure and function of formins

Formins are large (120–220 kDa) proteins that interact with many binding partners to perform their functions. Fungal species typically have 2 or 3 formin genes, whereas mammals have 15 and some plant species have more than 20 [44-46]. Formins are also implicated in a growing number of diseases [47-49]. Many members of formin families were isolated genetically through mutations causing disfunctions of the cytoskeleton [43]. The Bni1p (Bud neck involved 1 protein) formin was first identified by J. Pringle [50]. The knock-out mutation of this protein and that of Cdc12 (Cell division control protein 12) together is lethal in budding yeast. If Bni1 is mutated alone, there is a slight deficiency in the proliferation [51]. Some formins have additional effects on actin beyond nucleation and elongation. For example, *S. cerevisiae* Bnr1p (Bni1p related 1 protein), mouse mDia2, formin-like protein 1 (FMNL1; also known as FRL1), FMNL2 (also known as FRL2), FMNL3 (also known as FRL3) and *Arabidopsis thaliana* FH1 bundle actin filaments [52-55], whereas mouse FMNL1 and inverted formin 2 (INF2) and *A. thaliana* FH8 sever and/or depolymerize actin filaments [56-58]. Many cells express formins with overlapping functions. For example, the Bni1p formin of the *Saccharomyces cerevisiae* basically helps in the formation of actin bundles but in the absence of this formin, another one, the Bnr1p takes over its function [59].

It is recognized that the diaphanous protein from Drosophila, the Bni1p protein from fission yeast and the mammalian formins consist of two homologous sequences. The characteristic FH domains, of formins were first defined by Castrillon and Wasserman (*Fig. 5*).

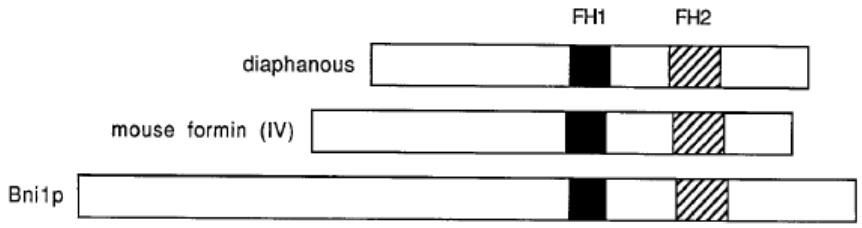

Figure 5 – First publication of the FH (formin homology) domains. The authors gave the name FH1 to the proline rich domain and FH2 to the most conserved amino acid region [60].

These FH domains occur in many proteins of different organisms. Most formins have both FH1 and FH2 domains with a functionally important linker region in-between. The FH1 domain consists of 5-12 repeating prolines (poly-L-proline chains) and are able to interact with profilin. The expressed FH1-FH2 region functions as an active formin in living cells [61-64]. The FH2 domain forms a head-to-tail doughnut-shaped dimer that closes around the barbed end of the actin filament. In mDia1 or mDia2, the linking sequence containing the FH2 domain binds directly to microtubules and interacts with three microtubule plus-end tracking proteins: the end-binding protein 1 (EB1; also known as MAPRE1), the adenomatous polyposis coli (APC) and the cytoplasmic linker protein 170 (CLIP170; also known as CLIP1) [65-67]. The FH2 domain is the most conservative unit and shows no sequence-similarity to other domains or polypeptides [31]. It binds the barbed end of an actin filament affecting the growth and serves protection against capping proteins [31]. It was thought previously that the FH2 domain contains approximately 100 amino acids [60]. According to the latest sequence analyses it is known that there are almost 500 amino acids in this region, including the C-terminal DAD (Diaphanous autoregulatory domain). If the C-terminal (containing the DAD domain) is deleted than the activity of the Bni1p decreases to the half [4].

According to the model of Zigmond [68], the FH2 domain is necessary and sufficient for the nucleation of actin and for the stabilization of actin dimers. FH2 is

also able to form oligomers. For example, FH2 subunits of Bni1p formin form dimers when they are crystallized, and they form tetramers in solutions [62, 68]). The first step of the formation of an FH2-actin dimer-complex is either the binding of a preformed actin dimer by a FH2 dimer or the FH2 dimer catches two actin monomers and helps them forming the nucleus as it is shown in *Fig. 6*.

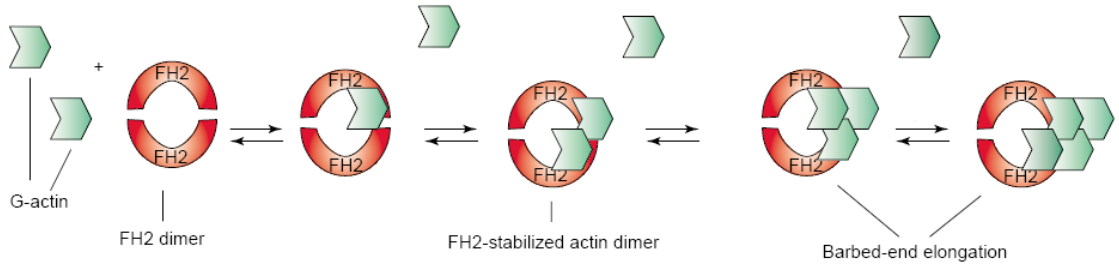

Figure 6 – Steps of actin nucleation by mDia1-FH2 dimer [31].

Once a filament is nucleated, the dimeric FH2 domain moves processively with the growing barbed end, protecting it from capping proteins, while allowing the rapid addition of new subunits [63, 68, 69]. The rate of FH2 movement correlates with the rate of actin subunit addition, which can exceed 100 subunits per second [69-71]. Each transition or 'step' that the FH2 domain makes might be triggered by the addition of the previous actin subunit [72]. The flexible linker region connecting the FH2 hemi-dimers plays a critical role in these events by accommodating drastic spatial rearrangements of the hemi-dimers with respect to each other, which is predicted to occur with each step [29].

The FH2 subunit must compete with other barbed end-binding proteins, e.g. CapZ homologues and gelsolin [73]. Which 'cap' will be able to cover an end of an actin filament? It depends on the relative concentrations of the different capping proteins and their affinities. Accordingly, in areas where formins are present at high concentration, their effect predominates (e.g. the Bni1p in yeasts are present at high concentration at the tip of the bud). The FH2 can decrease both the rate of polymerization and depolymerization. For example the Bni1p-FH2 domain partially inhibits depolymerisation at the barbed end even if the protomers bind ATP, ADP.P_i or ADP. When the FH2 concentration is enough to saturate each barbed end then the inhibiting effect is still just partial. After all, the FH2 domain is not a 'weak cap' at the

barbed end, rather it can be regarded as a 'leaky cap' that allows the polymerization at the barbed end when bound. Recent results showed that mDia1-FH1-FH2 accelerates the growth of an actin filament by 2 µm/second, corresponding to 720 actin monomers binding to the barbed end in one second [70]. This very fast process cannot take place by the quick attachment and detachment of FH2 domain, more likely this domain remains attached and quasi 'walking' with the end of the filament while it grows, as mentioned before. This process depends on the dimer- and multimer-forming ability of FH2 [31, 62, 68].

The FH3 domain is found in the N-terminal region in the members of formin families. This region is the least conserved and its functions are least known [74]. It is likely responsible for the specific binding of given structures (*Fig. 7* – arrangement of formin homology domains in several formins).

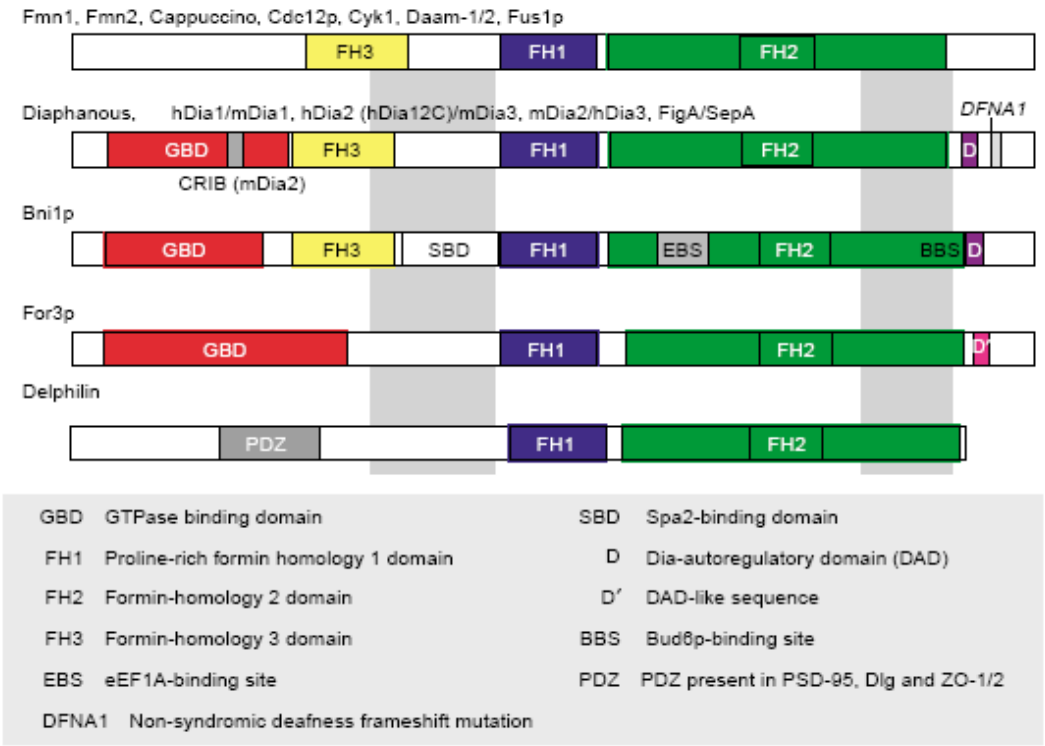

Figure 7 – Structure similarity of different formins with the highly conserved FH domains [75].

Many formins directly bind and regulate microtubules [76, 77]. This puts formins in an ideal position to coordinate functions which depend on the concerted action of the actin and microtubule cytoskeleton [78, 79]. Members of Dia, FMN and INF formin subfamilies have possible roles in microtubule regulation. But how do

mDia1 and mDia2 stabilize microtubules? Based on results from injecting cells with either mDia1 or mDia2 and fluorescent tubulin, each formin decreases the tubulin subunit exchange at microtubule plus ends [80] and both regulate the organisation of the cytoskeleton during mitosis and meiosis (e.g. mDia2 binds directly to microtubules of given cells *in vitro* [80], while mDia1 binds to the mitotic spindle of HeLa cells via its FH3 domain [81]).

1.2.2 The molecular regulation of formins

Many FH proteins were identified as small Rho GTPase effectors [82]. The Diaphanous-related formins (Drfs) are able to attach to activated small GTPases of GTP-binding Rho families through their N-terminal GTPase binding region (GTPase-binding domain (GBD) or Rho-binding domain (RBD)). For example, Rho1p, Rho3p and Rho4p can bind Cdc42p, whereas Rho3p and Rho4p can bind Bnr1p [83, 84]. The preferred activator of Bni1p is Rho3 but in the absence of Rho3, Rho4 is able to activate it as well. The mammalian homologue *Drosophila* diaphanous mDia is bound by RhoA [83-85]. Stress fibres can be induced in mammalian cells by the activation of mDia1 and mDia2 through Rho or, alternatively, by the activation of a third protein FHOD1 (formin homology 2 domain containing 1) through Rac [86-88]. The GTPase binding regions are not conserved and the process of binding is not yet known in Drfs families. First, Rho proteins must be locally activated by signals (e.g. chemoattractants, mating pheromones or growth factors) and then they can recruit downstream effectors, including formins, to remodel the cytoskeleton [89]. The Rho GTPases work as (binary) molecular switches: with an ‘on’ state, when they bind GTP and ‘off’ state after the hydrolysis of GTP to GDP (*Fig. 8*). For the state of GTPase GDP-GTP exchange factors (GEFs) are responsible which act by extracellular stimuli. Many signal transduction pathways are regulated by small GTPases, which basically act through the reorganization of actin and microtubule networks and the expression of new genes [90, 91]. The C-terminal of Drfs binds to the N-terminal of GTP-binding domain (GBD) by default, making the protein inactive. If a conserved C-terminal region (DAD) breaks this bond, the protein becomes active (*Fig. 8*) [92]. It is not completely known, which groups of formin family proteins are able to autoregulate. Though a few formin

contain GBD and DAD or DAD-like region, only mDia1 and mDia2 are capable of autoregulation through binding their N- and C-terminal domains [88, 92]. Deletion of either GBD or DAD sequences result in active formins [88, 92, 93].

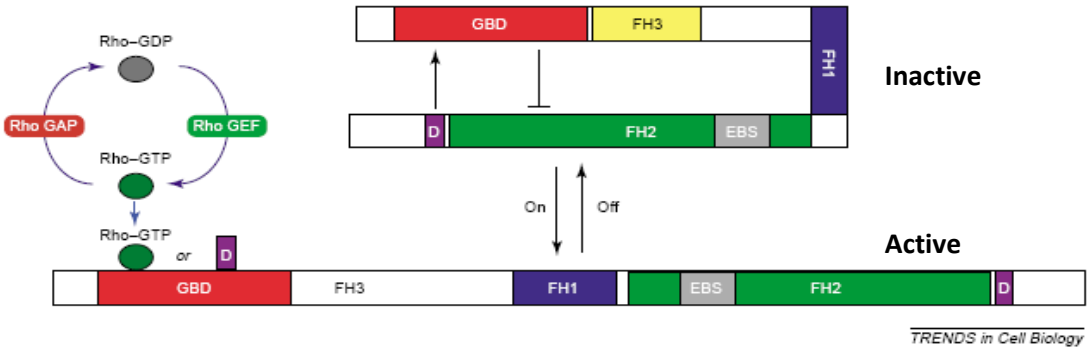

Figure 8 – Activation and inactivation of formins [75].

The Diaphanous-autoregulatory domain is a conserved protein region that can be separated into two main parts: a leucin-rich sequence similar to the WH2 subunit of the WASP/Scar family actin nucleation initializing factor, and a group of subunits required to fulfil the autoregulatory function. The DAD region of mDia2 did not interact with small GTPases, suggesting that it does not play a role in the activation of formins, and only has an autoregulatory function.

1.2.3 The interaction of formins with cytoskeletal proteins

Formins exert their greatest effect mostly on the actin cytoskeleton, which facilitating the formation of long unbranched filaments [63, 64]. The interaction between Bni1p and the actin-cytoskeleton was first observed when the FH1 domain of Bni1p was linked to an actin binding protein, profilin [50, 83]. Profilin is a G-actin binding protein, which interacts with several formin FH1 domains. Profilin plays an essential role in the cells, e.g. maintains the G-actin pool [94] and is required for cell division in the case of *C. elegans* and fission yeasts [95, 96]. Both Bni1p and Cdc12p formins bind to the barbed end of actin filaments and reduce the polymerization-depolymerisation rate by 50%. The overexpression of FH1-FH2 domains of Bni1p and Cdc12p yeast formins is

lethal because the amount of actin filaments increases excessively that perturbs the normal balance of treadmilling [61, 63, 64, 97].

Formins also control the polarization of microtubules in yeasts. For example, in *Schizosaccharomyces pombe* three formins take part in the formation of the cell shape and For3p is responsible for the formation of actin bundles and the organization of microtubules [98]. Cdc12p essentially regulates the formation of the contractile actomyosin ring during cell division [95], while Fus1p is a non-essential FH protein, which is required for the polarization of the actin network during sexual reproduction of certain cells [74].

The presence of the FH2 domain of the mDia1 is sufficient to increase the amount of F-actin in cells, although this effect is weaker than in the case when both FH1 and FH2 domains are present. To achieve the same effect with mDia2, its FH1 unit is indispensable. Diaphanous formins have another actin related effect: the activation of the serum response factor (SRF). This activation is performed through their actin regulating capability. SRF is a transcription factor that regulates the function of many serum-induced muscle-specific genes [91, 99, 100].

1.3 Tropomyosin

Tropomyosins (Tm) form a large family of protein isoforms, expressed from multiple genes. They are components of the thin filament, bind to the alpha-helical groove of the actin filament and play a very important role in the regulation of muscle contraction [101, 102]. Tropomyosins can be grouped according to their molecular weight, yielding high molecular weight (HMW – 284 amino acids) and low molecular weight (LMW – 248 amino acids) isoforms [103]. In non-muscle cells Tm isoforms have been implicated in several processes including cytokinesis, vesicle transport, motility, morphogenesis and cell transformation [101, 102, 104, 105]. Since it was discovered in 1948 [106] its role in the muscle contraction has been published many times, though the exact functions of tropomyosins in non-muscle cells have not exactly been determined yet.

The tropomyosin coiled-coil acquires a helical contour and thus represents a coiled coiled-coil. Tropomyosin molecules link end-to-end to form continuous strands, that are bound tightly along the surface of helically arranged actin protomers of thin filaments [107-110]. The conserved N-terminal region of α-tropomyosin plays a critical role in the function of the striated muscle. This region is the same in fruit fly (*Drosophila melanogaster*) and rabbit (*Oryctolagus cuniculus var. domestica*). If any amino acid is exchanged in this region, the affinity to actin and to troponin is lost [111]. The α and β isoforms have different structure and they differ in their functions as well. In normal mouse heart the α isoform is dominant and only traces of the β isoform can be found. Shifting of this proportion to 80% β isoform in transgenic mice is lethal before the second postnatal week [103]. As we normalize the proportion of the two isoforms towards the normal values the function of the heart is restored [112]. In skeletal and heart muscle tropomyosin forms a tight functional unit with troponin [113] (*Fig. 9*).

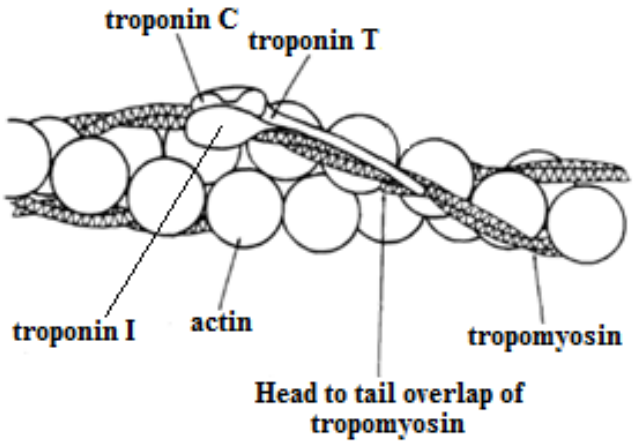

Figure 9 – Scheme of a skeletal muscle thin filament in rabbit [113].

There are four tropomyosin genes identified in mammals and birds (α, β, γ, δ), encoding for more than 24 isoforms [114] (*Fig. 10*). All four genes show extensive variation in isoform expression during muscle differentiation [115]. In brain, development is followed by widespread changes in isoform expression, and regional variation in expression is also seen. For example, the α-isoform α_f-Tm is restricted to cardiac and fast-twitch skeletal muscle, whereas α_s-Tm is present in slow-twitch

skeletal muscle [115, 116]. By contrast, the α-isoforms TmBr-1 and -3 are expressed in neurons [116-118].

Most isoforms are expressed in different cells and tissues, though the pattern of expression differs dynamically between different tissues [110, 119]. Qualitative and quantitative variation in the Tm content of actin filaments is therefore widespread and has the ability to contribute to specialized actin function in different cell types. Isoform-specific changes in tropomyosin expression have been commonly associated with cancer, including human primary tumors [120-125]. The reduction of expression of high-molecular-weight tropomyosins is very common in highly malignant cells [121, 123, 125, 126] and the increased expression of the cytoskeletal TmBr3 induces lamellipodia, increases cell movement and decreases the amount of stress fibres [127].

At least one essential Tm function in yeast involves vesicle transport from the Golgi to sites of polarized growth [128]. In *Caenorhabditis elegans*, elimination of the third and fourth isoforms of the tmy-1 gene affects development [129]. Deletion of the single known cytoskeletal Tm gene in *Drosophila melanogaster* results in altered head morphogenesis and different organization of the striated muscle contractile apparatus [130-132]. Similarly, knockout of one α-Tm isoform [133] or all α-Tm gene isoforms [134] in mice causes embryonic lethality at different embryonic stages. This suggests that cytoskeletal isoforms are required earlier for normal development, and the striated muscle isoform is required at a later stage.

The above examples illustrate some of the diverse function of Tms.

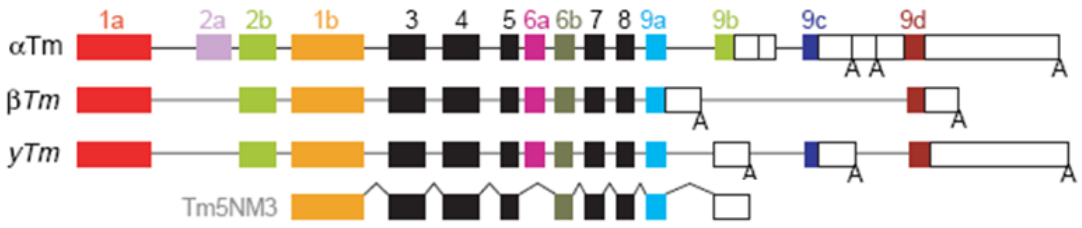

Figure 10 – Domain structure of a few tropomyosin isoforms [114].

In addition to these, recent studies showed that tropomyosins and formins are able to exert their protective effect on the actin filaments by inhibiting their fragmentation

[135]. The observation that Tm colocalizes with formin-induced actin filaments in living cells [95, 136-139] suggests that tropomyosin may regulate the conformation of flexible (formin-bound) actin.

1.4 Myosin and heavy meromyosin

The term myosin is used to refer to a diverse superfamily of molecular motors capable of translocating either actin filaments or other cargo on fixed actin filaments [140] (*Fig. 11*). The myosin superfamily consists of at least 35 different classes. The myosin II subfamily – which includes skeletal, cardiac and smooth muscle myosins, as well as nonmuscle myosin II (NMII) – is the largest [141] and the only class the members of which are capable of forming thick filaments at low ionic strength. The single-headed myosin I proteins were originally discovered in *Acanthamoeba* and are now expected to be ubiquitous in eukaryotes.

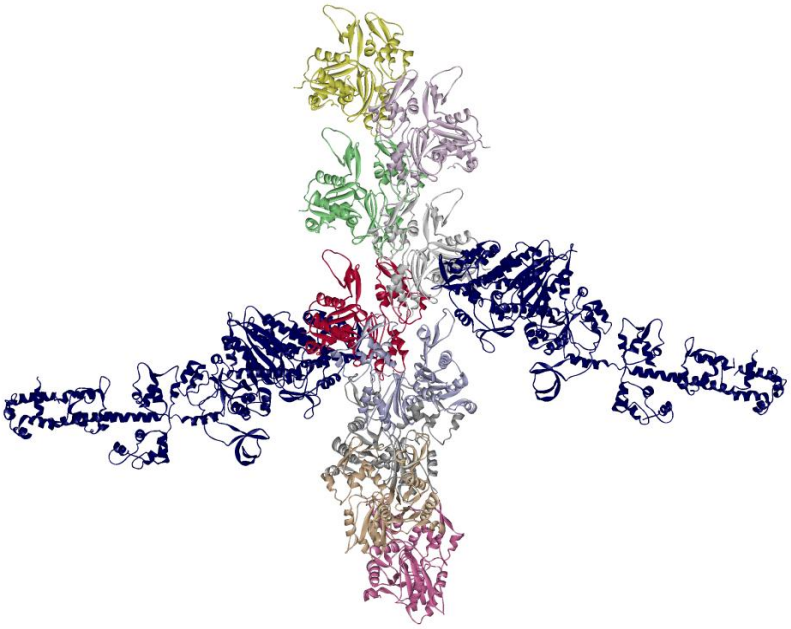

Figure 11 – Structural view of an actin filament (protomers with different colours) with bound myosin subfragment 1 (S1) (dark blue colour). The figure was created based on the pdb file *1MVW* [142].

Much less is known about the structure, function, and intracellular localization of the members of myosin classes III to XXXV. Many new myosins have been discovered in

the last few years thank to the application of PCR (polymerase chain reaction). The salient feature of all myosins is the ability to reversibly bind actin and hydrolyse ATP. Typically, the ATPase activity of myosin alone is very low and it is markedly increased by the interaction with actin [140]. In vertebrates, there are over 15 different myosin II isoforms, each of which contains a different myosin II heavy chain (MHC). All myosin II molecules are hexamers composed of MHC dimers and two pairs of myosin light chains. Although their contractile activity is most evident in differentiated muscle tissues, such as the beating heart, it is also observed in nonmuscle cells in diverse cellular processes such as cell division, cell migration, and cell-cell or cell-matrix adhesion [141].

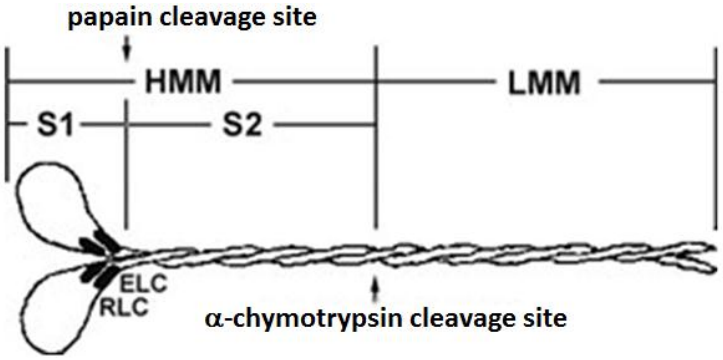

Figure 12 – Schematic representation of a myosin II dimer with papain and α-chymotrypsin enzymatic cleavage sites [143].

The proteolytic digestion of myosin II by α-chymotrypsin results in the so-called heavy meromyosin (HMM) that is commonly used in experimental work because of its solubility (*Fig. 12*). It consists of two motor domains which dimerise through an α-helical coiled coil.

2 Main objectives

It was shown by fluorescence spectroscopy that formin fragments have the ability to increase the flexibility of actin filaments through long-range allosteric interactions after binding to the barbed end of the filaments [144, 145]. These studies underlined the importance of the intramolecular conformational changes induced by formins in the structure of actin filaments. The generation of flexible actin filaments by formin binding can have a well-defined biological role, which is manifested under special intracellular conditions for particular functions. My aim was to find actin-binding proteins, which may have the ability to affect the formin-induced flexibility of actin filaments.

Formin-generated actin structures interact with many actin-binding proteins that can influence the formin-induced conformational transitions. One of these interacting proteins, tropomyosin, was shown to reverse the formin-induced conformational changes and stabilize the structure of the filaments [146]. Myosin is one of the most abundant actin-binding proteins that also localizes to formin-nucleated actin structures in cells [147, 148]. Myosin binding to actin filaments induces long-range allosteric and cooperative effects in the conformation of the filaments [149-152], which was shown to be dependent on the myosin isoform [153]. Thus, myosin can be another candidate for the regulation of the conformational dynamics of formin-nucleated actin structures. For these purposes fluorescence spectroscopy methods were applied. Our aim was to answer the following questions:

- How do the formin fragments influence the structure of actin filaments?
- What is the effect of tropomyosin on the flexibility of mDia1FH2-induced actin filaments?
- Is the effect of tropomyosin ionic strength dependent?
- Does heavy meromyosin affect the flexibility of formin-nucleated actin filaments?

3 Materials and methods

3.1 Materials

$CaCl_2$, KCl, $MgCl_2$, Tris, protease inhibitor cocktail, ammonium-sulphate ($(NH_4)_2SO_4$), glycogen, IAEDANS (N-(Iodoacetaminoethyl)-1-naphtylamine-5-sulfonic acid), IAF (5-(Iodoacetamido)fluorescein), EGTA, EDTA, phenylmethanesulphonyl fluoride (PMSF), dithiothreitol (DTT), sodium azide (NaN_3), α-chymotrypsin, ammonium sulphate, thrombin, ATP, IPTG (Isopropyl-beta-D-1-thiogalactopyranoside) and β-mercaptoethanol were obtained from Sigma Chemical Co. (St. Louis, MO, USA). dimethylsulphoxide (DMSO) was obtained from Fluka (Buchs, Switzerland). LB Broth and Agar Agar were from Scharlau (Debrecen, Hungary).

3.2 Protein preparation and purification

3.2.1 Actin

Acetone-dried powder of rabbit skeletal muscle was obtained using a preparation technique described previously [19]. First, ~360-370 g of *psoas major* muscle and the *longissimus dorsi* muscle of the euthanized and well bled rabbit were placed in ~350 ml cold distilled water, and then the muscle was ground two times. The ground muscle was placed in 1 liter of buffer 1 (0.15 M KH_2PO_4, 0.15 M K_2HPO_4, 0.1 M KCl – pH 6.5) and stirred with a glass rod for 15 minutes. After the stirring the liquor was filtered through 4 layers of gauze and the muscle was placed in 2 liters of buffer 2 (0.05 M $NaHCO_3$ – pH 6.5) and stirred with a glass rod for 10 minutes. This step was followed by another filtering with 4 layers of gauze. The muscle scone was then placed in 1 liter of buffer 3 (1 mM EDTA – pH 7.0), stirred for 10 minutes, and then filtered through 4 layers of gauze. 2 liters of distilled water was poured on the muscle piece and after 5 minutes of stirring the liquor was filtered through 4 layers of gauze. The last step with the distilled water wash was repeated. Next, the filtrate was washed 5 times for 5-10 minutes with 1 l of clean acetone with gentle stirring at room

temperature in a ventilated laboratory hood. Each step was followed by filtration through 4 layers of gauze. The muscle powder was dried overnight in the hood. On the next day the acetone-dried muscle powder was weighed and kept at -20 °C.

Rabbit skeletal muscle actin was prepared from acetone-dried muscle powder according to the method of Spudich and Watt [154]. Each gram of acetone-dried muscle powder was extracted by stirring in 20 ml buffer A containing 4 mM Tris-HCl (pH 7.3), 0.2 mM ATP, 0.1 mM $CaCl_2$, 0.5 mM DTT and 0.005 % NaN_3 at 4 °C. After 30 minutes of gentle stirring the liquor was filtered through 4 layers of gauze and the extraction step was repeated with the same volume of fresh buffer A. After the second filtration the filtered liquid was collected and polymerized at room temperature by the addition of 100 mM KCl and 2 mM $MgCl_2$. After 2 hours of polymerization 0.6 M solid KCl was added to the liquor which was gently stirred and kept at 4 °C for 30 minutes. When the KCl was completely dissolved the liquid was ultracentrifuged at 328,000×*g* for 30 minutes and the pellets were swollen on ice for at least 2 hours by the addition of given amount of buffer we needed for further procedures. The swollen pellets were gently homogenized and dialysed against the experimental buffer overnight at 4 °C. The concentration of G-actin was determined spectrophotometrically with the absorption coefficient of 0.63 mg ml^{-1} cm^{-1} at 290 nm [155]. A relative molecular mass of 42,300 was used for G-actin [156].

3.2.2 mDia1-FH2 formin fragment

The FH2 fragments of mammalian formin mDia1 (mDia1-FH2+linker) were prepared based on previously described methods [41, 144]. The mDia1 fragments were expressed as glutathione s-transferase fusion proteins in *Escherichia coli* BL21 (DE3)pLysS strain. After culture medium liquids and gels were made (25 g/l LB Broth, 2 % agar, 100 µg/ml ampicillin) 5 µl of mDia1-FH2 plasmid (pGex-4T2 with ampicillin resistance) was mixed with 100 µl competent cells and the mixture was kept on ice for 30 minutes. 42 °C water bath was applied as heat shock for 45 seconds and then the sample was placed back on ice. After 2 minutes the sample was mixed with 0.9 ml of preheated (37 °C) liquid culture medium and was kept at 37 °C for 2 hours, shaken with 200 rpm. Cells were spread on LB agar plates and incubated overnight at 37 °C.

150 ml of liquid culture medium was incubated with a single colony from the transformation and was shaken overnight at 37 °C, 120 rpm. Next morning 20-20 ml of cell culture was pipetted into 1-1 l of liquid culture medium (containing ampicillin) and the cells were grown for 2.5 hours at 37 °C (at 120 rpm). At OD 0.75 the temperature was decreased to 20 °C and the cells were induced overnight by adding IPTG to a final concentration of 0.3 mM. Cells were collected by centrifugation at 4,000 rpm, 4 °C for 20 minutes. Pellets were used immediately or were frozen in given aliquots and were kept at -20 °C for later use.

Protease inhibitor cocktail (43 mg Protease inhibitor was dissolved in 1 ml of mixture of DMSO and distilled water (200 µl DMSO and 800 µl dH_2O) and 1 ml cocktail was added per 4 g of cell pellets), 250 µl PMSF (from 100 mM stock solution) and approximately 50 ml of lysis buffer (50 mM TRIS-HCl (pH 7.6), 5 mM DTT, 5 mM EDTA, 1 mM PMSF, 50 mM NaCl, 10 % glicerol) were added to approx. 14-16 g of pellet. The mixture was homogenized on ice and was completed to approx. 130 ml with lysis buffer. Liquor was sonicated (Bandelin Sonoplus HD3100 with MS73 probe tip) 6 times one minute with one minute pauses between each run and then was ultracentrifuged (Sorvall ULTRA Pro 80, with T-1250 rotor) at 30,000 rpm, 4 °C for 1 hour. Supernatant was collected, and kept on ice after the addition of DNAse (1 ml from the given stock solution – 10 mM TRIS-HCl (pH 7.5), 5 mg/ml DNase, 50 mM NaCl, 1 mM DTT, 10 mM $MgCl_2$, 50 % glycerol). During cell extraction an affinity chromatography glutathione(GSH)-agarose column was equilibrated with lysis buffer (by applying Pharmacia LKB FPLC) and the sample was loaded on the column (first plateau appeared on the plotter) which was followed by lysis buffer again. When the first plateau was “washed down” on the plotter by the buffer, lysis buffer was exchanged to buffer Wash-I (50 mM TRIS-HCl (pH 7.6), 5 mM DTT, 400 mM NaCl, 10 % glicerol). After a quite narrow new peak on the paper of the plotter Wash-I was changed to buffer ATP (50 mM TRIS-HCl (pH 7.6), 5 mM DTT, 10 mM $MgCl_2$, 100 mM KCl, 0.25 mM ATP, 5 % glycerol). When an upper plateau appeared again buffer ATP was changed to Wash-II (50 mM TRIS-HCl (pH 7.6), 5 mM DTT, 5 mM $MgCl_2$, 10 mM KCl, 50 mM NaCl, 5 % glycerol) and after a few minutes the protein was cleaved overnight at 4 °C by thrombin (80 U/ml, solved in Wash-II buffer). Next day the column was eluted with buffer Wash-II and the fractions were collected. The pooled fractions were loaded on

Sephacryl S-300 column with gel filtration buffer (50 mM TRIS-HCl (pH 7.3), 5 mM DTT, 50 mM NaCl, 5 % glycerol) to get rid of contaminations. Purified fractions were pooled and concentrated with a Millipore Amicon ULTRA 10k centrifugal filter unit. The concentration of the protein was determined photometrically with the absorption coefficient of A_{280} = 21,680 M^{-1} cm^{-1} (ProtParam, http://us.expasy.org/tools/). The purified and concentrated protein was frozen in liquid nitrogen and stored at -80 °C in 50 µl aliquots. Purity of the protein was checked by SDS-PAGE. The formin concentrations are given as mDia1-FH2 monomer concentrations throughout this dissertation.

3.2.3 Tropomyosin

Tropomyosin was purified from rabbit skeletal muscle according to the procedure of Eisenberg and Kielley [157] and Smillie [158]. For the preparation we used the leftover scone of the muscle powder remained from an actin preparation. The scone was placed in a beaker and 100 ml of buffer 1 (5 mM TRIS, 1 M KCl, 0.5 mM DTT – pH 7.0) was poured on it. The liquor was stirred overnight on ice and filtered through 4 layers of gauze. The liquor was used for the further operations. The pH of the liquid was decreased to 4.6 by using 0.1 M HCl drop by drop. After this isoelectric precipitation the liquid became opaque, was stirred on ice for 30 minutes then centrifuged at 6,000×*g* for 20 minutes at 4 °C. After the centrifugation the pellet was dissolved in buffer 2 (5 mM TRIS, 1 M KCl, 0.5 mM DTT – pH 8.0). (The volume of buffer 2 is the 80 % of the initial volume we started the procedure with.) The pH of the liquid was then increased to 8.0 by the addition of 1 M KOH. After 30 minutes of stirring on ice the liquor was centrifuged for 10 minutes at 6,000×*g* at 4 °C. The next isoelectric precipitation was carried out with the supernatant. The pH was decreased down to 4.6 again with 0.1 M HCl and the solution was kept on ice for 30 minutes with stirring. After the centrifugation (20 minutes, 6,000×*g*, 4 °C), the pellet was dissolved in buffer 2 of 60 % of the initial volume then the pH was set back to 8.0 with KOH and was left on ice for 30 minutes with stirring. This was followed by another centrifugation (10 min, 6,000×*g*, 4 °C) and a third isoelectric precipitation. After 20 minutes of centrifugation the pellet was dissolved in buffer 3 (5 mM TRIS, 0.5 mM DTT – pH 8.0)

with 40 % of the initial volume. The pH was then brought back to pH 8.0 with 1 M KOH and stirred on ice for 30 minutes. After centrifugation (10 min., 6,000×*g*, 4 °C) ammonium-sulphate was given in the supernatant in 31.2 g/100 ml concentration while the pH was kept constant. The liquor was centrifuged (30 min., 11,000×*g*, 4 °C) and then ammonium-sulphate was added to the supernatant in 7.34 g/100 ml final concentration (pH was kept constant again) and was left on ice while stirred for 30 minutes. After the last centrifugation (60 min., 11,000×*g*, 4 °C) the pellet was dissolved in 6 ml of buffer 3 and then the concentration of the tropomyosin was determined photometrically using the absorption coefficient of ε_{278} = 0.29 ml mg^{-1} cm^{-1} [157].

3.2.4 Heavy meromyosin

Myosin and heavy meromyosin was prepared with the method described by Margossian and Lowey [159]. First, ~100 g of *longissimus dorsi* muscle of the euthanized rabbit were placed on ice then the muscle was ground. The ground muscle was extracted in3 ml/g extraction buffer (0.3 M KCl, 0.09 M KH_2PO_4, 0.06 M K_2HPO_4, 0.2 mM ATP, 0.2 mM DTT, 0.23 mM PMSF – pH 6.8) and was stirred by a glass rod. After 15 minutes of stirring the liquor was filtered through 4 layers of gauze. The filtered liquid was diluted again up to 10x of its volume with ice-cold water then was incubated overnight. The supernatant was discarded and the sediment was centrifuged (Sorvall ULTRA Pro 80, with T-1250 rotor at 3,000 rpm, 4 °C, 20 minutes). The pellet was dissolved in equal volumes of buffer B (2 M KCl, 1 mM DTT) and buffer C (0.5 M KH_2PO_4, 0.5 M K_2HPO_4). The liquor was diluted with ice-cold water up to 150 % of its volume and then was centrifuged (Sorvall ULTRA Pro 80, with T-1250 rotor at 20,000 rpm, 4 °C, 30 minutes). Supernatant was completed with 10x amount of ice-cold water and stirred for 15 minutes. This precipitation was followed by another centrifugation (Sorvall ULTRA Pro 80, with T-1250 rotor at 3,000 rpm, 4 °C, 20 minutes) and the pellet was solved in given amounts of B and C buffers then the solution was completed with 1 mM DTT and 1 mM $MgCl_2$. The next step was centrifugation with 100,000×*g* for one hour at 4 °C. The myosin-containing

supernatant can be frozen in 50 % glycerol added for further use or the preparation of HMM can be started immediately. A given amount of myosin solution was dialyzed overnight against digesting buffer (10 mM TRIS-HCl (pH 7.6), 0.6 M KCl, 2 mM $MgCl_2$, 1 mM DTT) at 4 °C, which was followed by centrifugation (328,000×*g* for 40 minutes at 4 °C). The concentration of the supernatant was determined photometrically and then it was diluted to a concentration of 4.5 mg/ml with digesting buffer. The temperature was increased slowly to 25 °C, and 0.05 mg/ml α-chymotrypsin was added to the solution. After 10 minutes the digestion was stopped by 0.2 mM PMSF, followed by an overnight dialysis (10 mM MOPS-KOH (pH 7.0), 30 mM KCl, 1 mM $MgCl_2$, 1 mM DTT). The solution was clarified by centrifugation (Sorvall ULTRA Pro 80, with T-1250 rotor at 30,000 rpm, 4 °C, 90 minutes) then HMM was dialyzed again against the experimental buffer (mostly buffer A) and clarified again. The concentration of HMM was determined spectrophotometrically using the absorption coefficient of 0.56 mg ml^{-1} cm^{-1} at 280 nm. The HMM concentrations given here are heavy meromyosin monomer concentrations.

3.3 Fluorescent labelling of actin

Actin was labelled with IAEDANS or IAF dyes at Cys^{374} according to the method of Miki and co-workers (*Fig. 13*) [160]. 2 mg/ml F-actin was incubated at room temperature for 2 hours in buffer A without DTT after the supplementation with 100 mM KCl and 2 mM $MgCl_2$. Then the sample was incubated with tenfold molar excess of IAEDANS at room temperature for 1 hour. The label was first dissolved in a small amount of (~50 µl) dimethylsulfoxide, then DTT free buffer A was added to the solution (drop by drop till 800-1000 µl) before being added to the protein. Labelling was terminated with 2 mM β-mercaptoethanol. After ultracentrifugation of the sample for 45 minutes at 328,000×*g* the pellet was incubated in small amount of (depending on the size of the pellet) buffer A for 2 hours and then the swollen filaments were gently homogenized with a homogenizer. The homogenized sample was dialyzed overnight against buffer A at 4 °C which was followed by a clarification centrifugation (328,000×*g*, 30 minutes, 4 °C). The concentration of the fluorescent dye in the protein

solution (supernatant) was determined by using the absorption coefficient of 6100 M^{-1} cm^{-1} at 336 nm for actin-bound IAEDANS [161]. The extent of labelling was 0.8 – 0.9 mol/mol of actin monomer.

Labelling the Cys^{374} with IAF was prepared according to standard procedures [162, 163]. The monomeric actin (46 µM) was labelled in DTT free buffer A with a fifteen-fold molar excess of IAF which was dissolved in 0.1 N NaOH and added to the actin solution drop by drop at room temperature while the pH was kept constant with 0.1 N HCl. Afterwards the sample was incubated at 4 °C for 24 hours. After this incubation period the actin was polymerized for two hours at room temperature and then centrifuged at 328,000×*g* for 45 minutes at 4 °C. The pellet was treated in a similar way to that described in the case of labelling with IAEDANS. The concentration of the probe was determined using the absorption coefficient 60,000 M^{-1} cm^{-1} at 495 nm. The molar ratio of the bound probe to the actin concentration was 0.6–0.7.

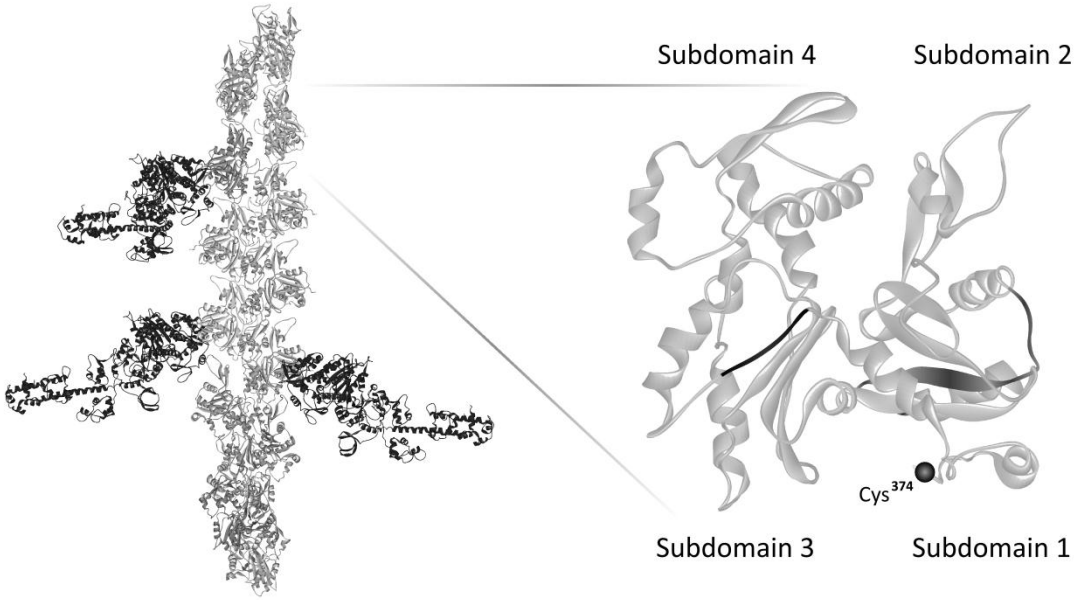

Figure 13 – The left panel shows a schematic representation of an actin filament decorated with myosin S1 fragments (created based on pdb file *1MVW*) showing fourteen protomers. The right panel shows a magnified view of an actin monomer (pdb file *2ZWH*) indicating the four subdomains with the Tm (left one; in subdomain 3) and HMM (right one; in subdomain 1) binding sites and the position of the fluorescent labels used in this thesis at the Cys^{374} [164].

3.4 Sample preparation

Preparations of the samples were made in the same way for both steady-state and anisotropy decay measurements each time unless stated otherwise. Buffer A and the unlabelled/labelled G-actin were added to quartz cuvettes and 0.2 mM EGTA and 0.05 mM $MgCl_2$ was added (final concentrations) to initiate the exchange of the actin-bound calcium for magnesium. 5-10 minutes later formin, formin and tropomyosin, formin and heavy meromyosin or just Tm or HMM (or e.g. in the case of control experiments their buffers were given alone) was added and the final concentration of $MgCl_2$ and KCl was adjusted to the given salt concentration to initiate the polymerization of actin. The total amount of sample was usually 1 ml or 100 µl when micro cuvettes were used. Most of the samples were incubated overnight at 4 °C in the dark and before the measurements they were kept at room temperature for at least 30 minutes. For some steady-state fluorescent anisotropy measurements the samples were measured right after they had been prepared.

3.5 Co-sedimentation assays

To characterise the binding of formin to actin filaments, actin (5 µM; 200 µl) was polymerized overnight at 4 °C as in the absence or presence of various mDia1-FH2 concentrations ranging from 0 to 5 µM. The samples were then centrifuged at 400,000 ×*g* for 30 min at 20 °C with a Beckman Optima MAX ultracentrifuge and a TLA-100 rotor. The supernatants were separated from the pellets, and the pellets were resuspended in 200 µl of buffer A. 100 µl Laemmli solution was added to the supernatants and to the resuspended pellets and then they were applied to a denaturing 12 % SDS-polyacrylamide gel which was stained with Coomassie Blue after electrophoretic run. The given protein band intensities were determined with a Syngene Bio-Imaging system.

3.6 Temperature-dependent Förster-type resonance energy transfer (FRET) experiments

These fluorescence measurements were carried out with Horiba Jobin Yvon Fluorolog-3 and PerkinElmer LS50B Luminescence Spectrometers, both equipped with a thermostated sample holder. To calculate the FRET efficiency the fluorescence intensities of the donor (IAEDANS) were recorded in the presence and absence of the acceptor (IAF). The excitation wavelength for IAEDANS was 350 nm. The optical slits on both sides were set to a value which serves quite high intensity values but does not cause photobleaching (typically 5 nm). During the measurements the emission spectra of the fluorophores were recorded between 370-550 nm and the integral of the 440-460 nm range was used for the calculations (that range is the peak of the donor emission spectrum). The fluorescence intensities were corrected for inner filter effect [165]. The FRET efficiency (E) was calculated as:

$$E = 1 - (F_{DA} / F_{D}) \quad (1)$$

where F_{DA} and F_{D} are the integrated fluorescence intensities of the donor molecule in the presence and in the absence of the acceptors, respectively. The value of E was determined at different temperatures between 6 and 34 °C, and a special FRET parameter, the normalized FRET efficiency (f'), was calculated using:

$$f' = E / F_{DA} \quad (2)$$

The temperature dependence of the f' can be informative about the flexibility of the investigated protein [166, 167]. For the interpretation of the FRET results, the temperature dependence of the relative f', defined as the value of f' at the given temperature divided by the value at the lowest temperature (6 °C) is presented. The larger temperature induced changes in the value of the normalized FRET efficiency are indicative for a more flexible protein matrix [166, 167]. Relative f' was measured at 10 µM actin (1 : 9 = donor : acceptor) with 500 nM formin in the case of tropomyosin-

effect examinations and at 5 µM actin (1 : 9 = donor : acceptor) with 500 nM formin in the case of heavy meromyosin-effect investigations.

3.7 Steady-state anisotropy measurements

These measurements were made with Horiba Jobin Yvon Fluorolog-3 fluorometer at 22 °C. The IAEDANS-labelled actin containing samples were irradiated with plane-polarized light at 350 nm wavelength, and the degree of polarization of the emitted fluorescence was analysed at 470 nm. Those fluorophores can be excited that are aligned in the plane of the incident radiation and they are able to emit fluorescence only. In the time interval between the absorption and the emission, the molecule can move out of the plane of polarization, so the emitted radiation will be depolarized to a degree that depends on the extent to which the molecule has moved. Small molecules and flexible protein matrices are moving faster and the degree of depolarization is higher than in the case of stiff, rigid protein structures. That is why this method was very efficient to determine the effects of different actin-binding proteins and environmental conditions on formin-mediated, flexible actin structures.

The kinetics of the change in the steady-state anisotropy ($r_{ss}(t)$) was analysed by fitting an exponential function to the experimental data using the following equation:

$$r_{ss}(t) = r_{max} - \Delta r * \exp(-k_{obs} * t) \qquad (3)$$

where r_{max} is the final (maximum) anisotropy, Δr is the difference between the initial and final anisotropy (anisotropy increase), t is the time and k_{obs} is the rate constant of anisotropy increase. For further analysis Δr or k_{obs} were plotted as the function of the HMM or TM concentration and fitted by a hyperbolic function using the following equation:

$$y = MAX \frac{c}{K_{1/2} + c} \qquad (4)$$

where MAX is the maximum increase of Δr or k_{obs} obtained at saturating amount of HMM or TM, $K_{1/2}$ is the half saturating concentration and c is the concentration of HMM or TM. Steady-state anisotropy measurements were usually made at 5 µM actin concentration. The concentration of the other actin-binding proteins was depending on the given experiment.

3.8 Steady-state fluorescence quenching experiments

Quenching experiments were carried out on a PerkinElmer LS50B Luminescence Spectrometer at 22 °C with 5 µM concentration of IAEDANS-labelled actin. The excitation wavelength was set to 350 nm and the emission was monitored through a wavelength range of 466-476 nm. The optical slits were set to 5 nm in both the excitation and emission paths. The acrylamide concentration was increased up to 0.5 M in subsequent steps during the measurements. The experiments were carried out in the presence of 1 mM $MgCl_2$ and 50 mM KCl (higher ionic strength) or 0.5 mM $MgCl_2$ and 10 mM KCl (lower ionic strength). The steady-state fluorescence quenching data were first analysed by using the classical Stern-Volmer equation [168]:

$$\frac{F_0}{F} = 1 + K_{SV}[Q] \tag{5}$$

where the F_0 is the fluorescence intensity of the fluorophore in the absence of quencher and F is the fluorescence intensity at varying quencher concentrations $[Q]$. The modified form of the classical Stern-Volmer relation (the Lehrer equation) was used when the samples contained more than one fluorophore population with different accessibilities [169]:

$$\frac{F_0}{\Delta F} = \frac{F_0}{F_0 - F} = \frac{1}{\alpha K_{SV}[Q]} + \frac{1}{\alpha} \tag{6}$$

where α is the fraction of the accessible fluorophore population.

3.9 Fluorescence lifetime-quenching measurements

Lifetime-quenching measurements were done at 22 °C with an ISS K2 multifrequency phase fluorometer (ISS Fluorescence Instrumentation, Champaign, IL). Sinusoidally modulated light (350 nm) from a 300 W Xe arc lamp was used for excitation and the emission was monitored through a 385FG03-25 high-pass filter. The modulation frequency was changed in 10 steps from 5 to 80 MHz. The data were analysed by ISS187 decay analysis software. All data were fitted to double exponential decay curves assuming a constant, frequency-independent error in both phase angle (± 0.200°) and modulation ratio (± 0.004). The goodness of the fit was determined from the value of the reduced χ^2 [170]. Average fluorescence lifetimes were calculated assuming discrete lifetime distributions [170]:

$$\tau_{aver} = \frac{\alpha_1\tau_1^2 + \alpha_2\tau_2^2}{\alpha_1\tau_1 + \alpha_2\tau_2} \qquad (7)$$

where τ_{aver} is the average fluorescence lifetime and α_i and τ_i are the individual amplitudes and lifetimes, respectively. The experiments were done with 20 µM actin in the presence of 0.5 mM $MgCl_2$ and 10 mM KCl.

The time dependent fluorescence quenching results were analysed with equations 3 and 4 by replacing the intensities with the corresponding fluorescence lifetimes [168].

3.10 Fluorescence lifetime and emission anisotropy decay measurements

The time dependent fluorescence measurements were carried out with the same ISS K2 multifrequency phase fluorometer using the frequency cross-correlation method. The excitation light was modulated with a double-crystal Pockels cell. Excitation wavelength was set to 350 nm and the emission was monitored through a 385FG03-25 high-pass filter. The modulation frequency was changed in 10 steps (linearly distributed on a logarithmic scale) from 5 to 80 MHz during the fluorescence lifetime measurements and in 15 steps from 2 to 100 MHz when anisotropy decays

were measured. Freshly prepared glycogen solution was used as a reference (lifetime = 0 ns). The fluorescence lifetimes of the fluorophore were determined by the use of nonlinear least-square analysis. The data were analysed by ISS187 and Vinci 1.6 decay analysis software. In fluorescence lifetime measurements all data were fit to double exponential decay curves assuming a constant, frequency-independent error in both phase angle (± 0.200°) and modulation ratio (± 0.004) (*Fig. 19*). The goodness of fit was determined from the value of the reduced χ^2 probe [170]. Average fluorescence lifetimes (τ_{aver}) were determined from the results of the analysis assuming discrete lifetime distribution with equation 7, where α_i and τ_i are the individual amplitudes and lifetimes, respectively [170]. The anisotropy is expected to decay as a sum of exponentials [171]. The experimentally obtained data were fitted to a double exponential function:

$$r(t) = r_1 \exp(-t / \varphi_1) + r_2 \exp(-t / \varphi_2) \qquad (8)$$

where φ_1 and φ_2 are rotational correlation times with amplitudes r_1 and r_2. The concentration of actin was 30 µM (1.3 mg/ml) during the fluorescence anisotropy decay measurements except where indicated otherwise. The experiments were carried out in the presence of 1 mM $MgCl_2$ and 50 mM KCl, unless stated otherwise.

Actin binding proteins often exert their effects on the conformation of actin filaments cooperatively. Cooperativity in this case means that the binding of a partner molecule can change the conformation of actin protomers distant from the binding site. One way of describing this cooperative effect is to define a cooperative unit, i.e. the set of actin protomers which are affected by the binding of one partner molecule. In this work we estimated the length of the cooperative unit using the linear lattice model and the following equation [150]:

$$p = p_1 - (p_1 - p_2)(1 - \alpha)^N \qquad (9)$$

where p is either the longer rotational correlation time from anisotropy decay experiments, or the value of the relative f' at the highest applied temperature

(defined here as actin flexibility). *N* is the length of the cooperative unit, p_1 and p_2 denote the limiting values of the corresponding parameters obtained in the absence of myosin and at saturating myosin concentrations, respectively, and α is the binding density of myosin to actin. *Equation 9* was used to fit the experimental data to obtain the values for *N* (*Fig. 18* and *Fig. 23*). Note, that this equation allowed the application of the fits below $\alpha = 1$. As in strong-binding states the binding of HMM to actin is tight, we take the value of α as the myosin head : actin monomer concentration ratio. Due to this approximation the *N* values obtained from these fits somewhat underestimate the lengths of the cooperative units.

4 Results and discussion

4.1 The effect of mDia1-FH2 on the structure of actin studied by fluorescence quenching

Previous studies on the effect of the mDia1-FH2 formin fragment on the structure of actin filaments showed that the structure of formin-bound filaments differs from those polymerized in the absence of formins. Binding of mDia1-FH2 to the barbed ends of filaments made the structure of actin filaments more flexible, while side-binding of formins stabilised the filament conformation [145]. Based on these results first we wanted to explore the conformational changes in the actin filaments induced by formin binding. Steady-state and time-dependent fluorescence quenching proved to be the most informative methods for our investigations. We applied acrylamide as a neutral quencher and characterised the accessibility of the IAEDANS label attached covalently to Cys^{374} of actin protomers (*Fig. 13*). In the absence of acrylamide the fluorescence emission intensity of IAEDANS was slightly lower in the presence of formin than in its absence (*Fig. 14A*) suggesting that the binding of the FH2 domain changed the microenvironment of the fluorophore in the subdomain 1. Addition of acrylamide decreased the fluorescence emission of IAEDANS labelled actin filaments independently of the presence of formin (*Fig. 14A*). Analysis of primary data using the classical Stern-Volmer equation (*Eq. 5*) resulted in a linear plot in the absence, but a non-linear plot in the presence of mDia1-FH2 (*Fig. 14B*). For this reason the evaluation of the experimental data was performed with the modified Stern-Volmer (or Lehrer) equation (*Eq. 6*), which gave linear plots in both cases. In the absence of formin fitting the data with *equation 5* and *equation 6* gave K_{SV} value of $2.3 \pm 0.1\ M^{-1}$ (*Fig. 14B* and *14C*). In the presence of mDia1-FH2 the data analysis with the modified Stern-Volmer equation gave a K_{SV} value of $6.2 \pm 0.1\ M^{-1}$ (*Fig. 14C*). Using *equation 6* we are able to evaluate the experimental data even when the quenching processes are more complex. The fraction of the quenchable fluorophore population (α) was calculated as the inverse of the y-intercept. This value was 99 % in the absence of formins indicating that all fluorophores were accessible for the quencher. These observations are in

agreement with the results evaluated by *equation 5* (*Fig. 14B*) and also with the data from previous quenching studies on actin filaments [144, 172, 173].

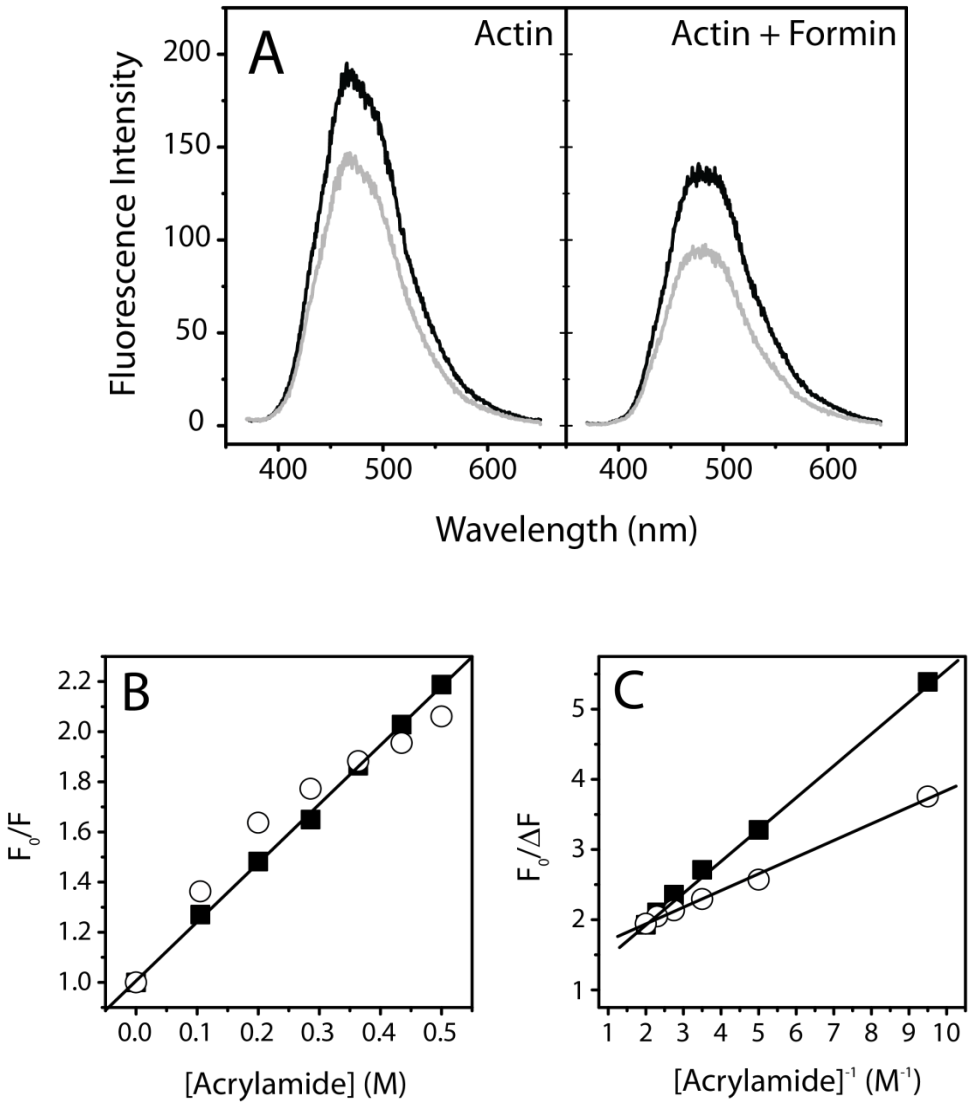

Figure 14 – Acrylamide quenching of the steady-state fluorescence emission of IAEDANS-labelled actin filaments. (**A**) Fluorescence intensity as a function of wavelength. Black curves show initial intensities for 5 µM actin filaments while gray curves show IAEDANS intensities after the addition of 0.1 mM acrylamide. 5 µM IAEDANS-labelled actin filaments in the absence (left panel) or in the presence (right panel) of mDia1-FH2 (500 nM). (**B**) Classical Stern-Volmer plot for formin-free actin filaments (filled squares), and for the filaments in the presence of 500 nM mDia1-FH2 (empty circles). Linear fit to the data (*Eq. 5*) obtained in the absence of formins gave K_{SV} value of 2.3 ± 0.1 M^{-1}. (**C**) Modified Stern-Volmer plots for actin filaments in the absence (filled squares) and in the presence (empty circles) of formin (500 nM). Fit using *equation 6* gave K_{SV} values of 2.3 ± 0.1 M^{-1} and 6.2 ± 0.1 M^{-1} for filaments in the absence and presence of formin, respectively. The corresponding α values were 93 ± 4 % and 68 ± 4 %.

The analyses with the Lehrer equation (*Eq. 6*) showed increase in the value of K_{SV} when formin was added to the samples. At 500 nM mDia1-FH2 concentration the K_{SV} was approximately three times larger (5.8 ± 0.1 M^{-1}) than in the absence of formins (*Fig. 15*), while the fraction of the quenchable fluorophores (α) decreased to 71 % (*Fig. 16A*).

To study the dependence of the observed effect the experiments were repeated at various formin concentrations and the data showed formin concentration dependence, i.e. the effect of formin depended on the formin : actin concentration ratio. The highest K_{SV} was observed at around 500 nM formin, above this concentration the value of K_{SV} decreased (*Fig. 15*), and at 3 μM formin concentration the value of K_{SV} (2.2 ± 0.1 M^{-1}) was similar to the initial value we obtained in the absence of formins (2.3 ± 0.1 M^{-1}). The formin concentration dependence of the fraction of the quenchable fluorophore population (α) followed opposite tendency, it was the lowest when the K_{SV} reached its maximum (*Fig. 16B*).

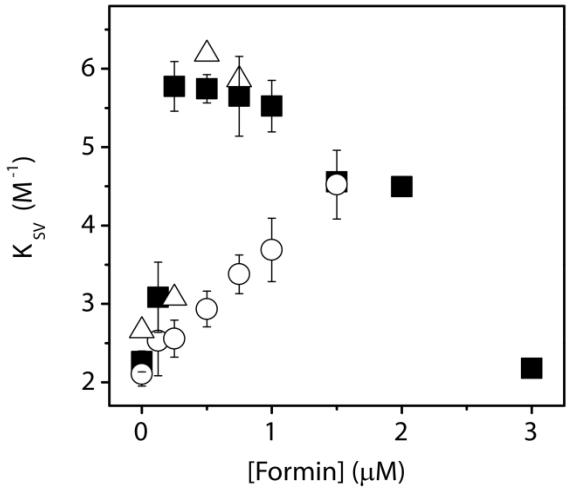

Figure 15 – Dependence of the K_{SV} values obtained from the modified Stern-Volmer analyses on the formin concentration. Salt concentrations were 10 mM KCl and 0.5 mM $MgCl_2$ (filled squares and empty triangles) or 50 mM KCl and 1 mM $MgCl_2$ (empty circles). The data for filled squares and empty circles were obtained from steady-state measurements while empty triangles are from fluorescence lifetime measurements.

The quenching experiments described above were carried out at 10 mM KCl and 0.5 mM $MgCl_2$ salt concentrations. Our previous results have shown that the effect of formins on the conformation of actin filaments depends on the ionic strength [144-146]. To further explore this effect we carried out the steady-state quenching

experiments at higher ionic strength (50 mM KCl and 1 mM $MgCl_2$) as well, to test whether quenching was sensitive to the salt concentration. In the absence of formins the value of K_{SV} measured at this higher salt concentration ($2.1 \pm 0.15\ M^{-1}$) was similar to that observed at lower ionic strength ($2.3 \pm 0.1\ M^{-1}$). At 500 nM formin concentration the K_{SV} was $2.9 \pm 0.2\ M^{-1}$ and the fraction of quenchable fluorophores decreased to 84 ± 3 %. At different salt concentrations the shape of formin concentration dependence of the quenching parameters was different as well (*Fig. 15* and *Fig. 16*). Within the applied formin concentration range neither the value of the quenching constant (K_{SV}) nor the fraction of quenchable fluorophores (α) had an extreme value, indicating that the interaction of formin with actin, thus their effects on the actin filaments depended on the ionic strength.

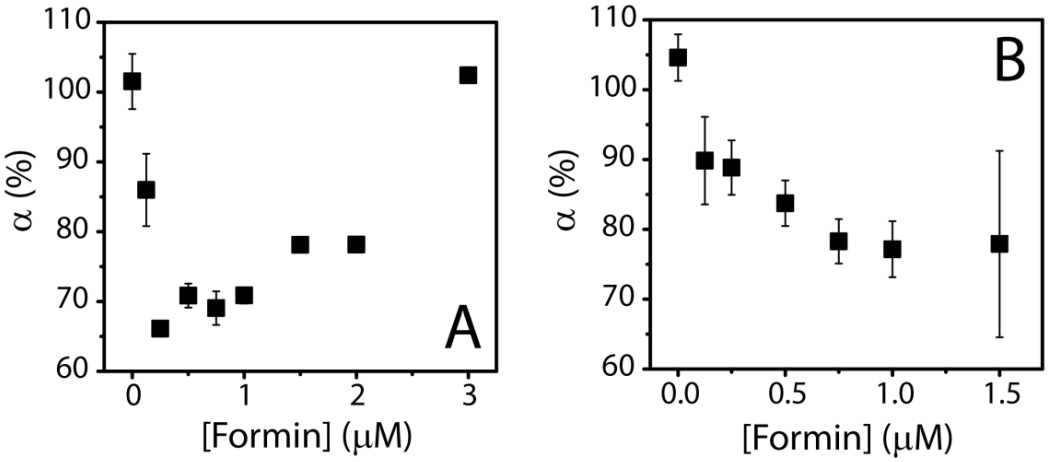

Figure 16 – Dependence of the fraction of fluorophores accessible for the quencher (α) on the formin concentration. The figure shows results obtained at 10 mM KCl and 0.5 mM $MgCl_2$ (**A**) or at 50 mM KCl and 1 mM $MgCl_2$ (**B**).

To test the magnitude of the contribution of static quenching mechanisms the dependence of fluorescence lifetimes on the acrylamide concentration in the absence and presence of formin were measured. These experiments were made under low salt conditions (10 mM KCl and 0.5 mM $MgCl_2$). The classical Stern-Volmer plot was linear in the absence of formin and gave a K_{SV} value of $2.6 \pm 0.3\ M^{-1}$, which is close to the value obtained from steady-state experiments ($2.3 \pm 0.1\ M^{-1}$) (*Fig. 15*). In the presence of mDia1-FH2 the classical Stern-Volmer plots were not linear, hence we applied the

modified Stern-Volmer equation to interpret the results. When 500 nM formin was added to the sample the K_{SV} increased to 6.2 ± 0.1 M^{-1}, to a similar extent that was observed in the case of steady-state measurements (5.8 ± 0.1 M^{-1}) under similar conditions (*Fig. 15*) and the fraction of quenchable fluorophores decreased to 53 %. There is a good agreement between the K_{SV} values from steady-state and time-dependent quenching results, indicating that the contribution of the static quenching mechanisms to the overall quenching process is negligible.

To exclude the contribution of fluorescence lifetime on the value of K_{SV} we measured the average fluorescence lifetime of the unquenched actin-bound IAEDANS resulting in 19.6 ± 0.6 ns and 18.9 ± 0.8 ns in the absence and presence of formin (500 nM), respectively. This small formin effect indicated that the change of the fluorescence lifetime could not account for the observed formin induced differences in the value of K_{SV}.

4.2 Study of the formin-induced changes in actin using FRET

To describe the effects of skeletal muscle tropomyosin and heavy meromyosin on formin-bound actin filaments we applied steady-state and time dependent fluorescence methods. As full-length myosin precipitates at relatively low ionic strengths (i.e. under the experimental conditions applied here) we used myosin fragments for the investigations. First we attempted to measure the effect of S1 in nucleotide-free solutions, where the actin binding affinity of S1 is high enough to achieve a high degree of saturation at moderate S1 concentrations. However, we observed that in the absence of nucleotides the effect of formins on actin filaments was hardly or not apparent. This observation is in line with previous findings that nucleotides play an important role in the interaction of actin with formin [73, 174]. Therefore, the use of nucleotides was necessary to assess the effect of myosin on the structure of formin-bound actin filaments. In the presence of ADP, the affinity of S1 for actin is relatively low, which made the saturation of actin with S1 problematic. To overcome this problem we applied double-headed heavy meromyosin, which has a substantially higher affinity for actin than S1 due to the possibility of simultaneous binding of two heads to adjacent sites of the actin filament [175]. This way we could

achieve a high degree of saturation of the myosin binding sites on actin even in the presence of ADP without the use of very high protein concentrations.

The first technique we used was the same temperature dependent FRET method we applied previously to study the effect of formin on the flexibility of actin filaments [144, 145]. Using this method we were able to characterize the effect of tropomyosin and heavy meromyosin on the dynamic properties of the formin-bound actin filaments. The donor and acceptor probes (IAEDANS and IAF) were attached to the Cys^{374} of actin protomers and the temperature dependence of the FRET efficiency was determined between 6 ^{o}C and 34 ^{o}C. Since only one fluorophore was bound to each protomer, the FRET was occurred between probes on neighbouring protomers, enabling us to caracterize the inter-protomer flexibility of actin filaments. If the temperature dependence of the normalized FRET efficiency (*Eq. 2*) is steeper in these experiments, it indicates that the protein matrix is more flexible between the donor and acceptor probes [166, 167]. Control experiments were made first and the relative *f'* (*Eq. 2*), was determined for actin alone at 5 µM and 10 µM actin concentrations. The results showed approx. 120-125% increase of the relative *f'* over the temperature range of 6 ^{o}C - 34 ^{o}C (*Fig. 17*). In the presence of 500 nM mDia1-FH2 the temperature profile of the relative *f'* became much steeper (increased to approx. 330-335%) indicating that the binding of formin changed the conformation of the actin filaments by making them more flexible (*Fig. 17*). This is in agreement with the results described in the previous chapter as well as with our previous observations [144].

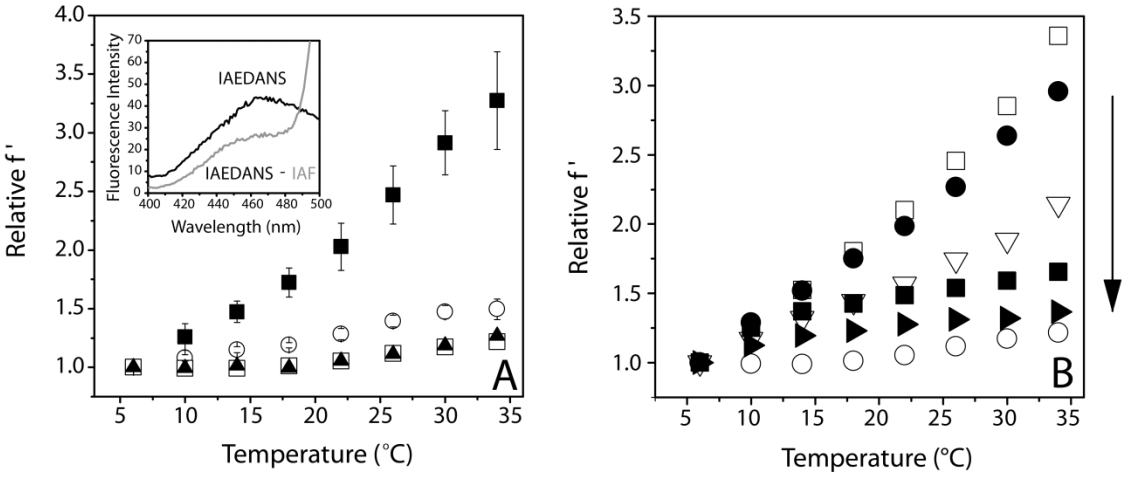

Figure 17 – Temperature dependence of the normalized FRET efficiency (relative *f'*, flexibility) for actin filaments. (**A**) Tropomyosin decreases the flexibility of formin-bound actin filaments. The experiments were carried out with 10 µM actin in the absence of actin-binding proteins (empty squares), or in the presence of mDia1-FH2 (500 nM; filled squares). The data obtained in the presence of tropomyosin (2 µM) and in the absence (filled triangles) or presence (empty circles) of 500 nM formin are also shown. The errors presented are standard errors from at least three independent experiments. The inset shows the fluorescence intensity of the donor measured in the absence of actin-binding proteins. The data were obtained in the absence (IAEDANS) or in the presence (IAEDANS-IAF) of the acceptor (as indicated). (**B**) Heavy meromyosin decreases the flexibility of formin-bound actin filaments. The experiments were carried out with 5 µM actin in the absence of actin-binding proteins (empty circles). Empty squares represent the data with 500 nM mDia1-FH2 in the absence of HMM. The data obtained in the presence of 500 nM formin and 1 µM (filled circles), 3 µM (empty triangles), 5 µM (filled squares) or 10 µM (filled triangles) skeletal muscle heavy meromyosin are also shown. Arrow in the right indicates the increase of the HMM concentration.

The buffer conditions of the experiments were 4 mM Tris-HCl (pH 7.3), 0.2 mM ATP, 0.1 mM $CaCl_2$, 0.5 mM DTT, 0.2 mM EGTA, 1 mM $MgCl_2$ and 50 mM KCl.

4.2.1 The effect of tropomyosin measured by FRET

To describe the effect of tropomyosin, skeletal muscle tropomyosin was added to the formin-bound actin filaments at 2 µM concentration. In the case of this isoform of tropomyosin, one molecule of tropomyosin binds to seven actin protomers on the filaments. Considering that under these conditions the affinity of tropomyosin for the actin filaments is ~0.5 µM [176] 2 µM tropomyosin is able to saturate the tropomyosin binding-sites on actin with a concentration of 10 µM. When formin and tropomyosin were both present, the value of relative *f'* increased to 150 % over the investigated temperature range (*Fig. 17A*). This tendency was similar to that observed in the absence of formin and tropomyosin, or in the presence of tropomyosin only

(*Fig. 17A*). This observation indicates that tropomyosin makes the formin-bound actin filaments more stable, and this stiffer conformation is similar to that observed in the absence of formin and tropomyosin.

4.2.2 The effect of heavy meromyosin measured by FRET

To show the effect of myosin, skHMM (skeletal muscle heavy meromyosin) was added to the formin-bound actin filaments at different concentrations. The results showed that HMM decreased the effect of the mDia1-FH2. The temperature dependence of the relative *f'* depended on HMM concentration. When the concentration of HMM heads was the same as the actin concentration (5 μM) the increase of the relative *f'* was 65 %, while at HMM concentration two-fold higher than the actin concentration the relative *f'* changed by 36 %. *Figure 17* summarizes the HMM concentration dependence of the FRET data assuming that the value of the relative *f'* at the highest temperature (34 ^{o}C) characterizes the flexibility of the actin filaments. These observations suggested that the formin-induced increase of the flexibility of actin filaments was reversed by the binding of HMM (*Fig. 17B* and *18*). To estimate the length of the cooperative unit we used *equation 9* to fit the data in *Figure 18*. The value of this parameter was found to be 1.3 $\pm$ 0.1, which is somewhat smaller than the one we obtained from the anisotropy decay experiments (2.0 $\pm$ 0.3; *Fig. 23*), indicating that the two methods are sensitive to different conformational transitions and modes of motion of the actin filaments.

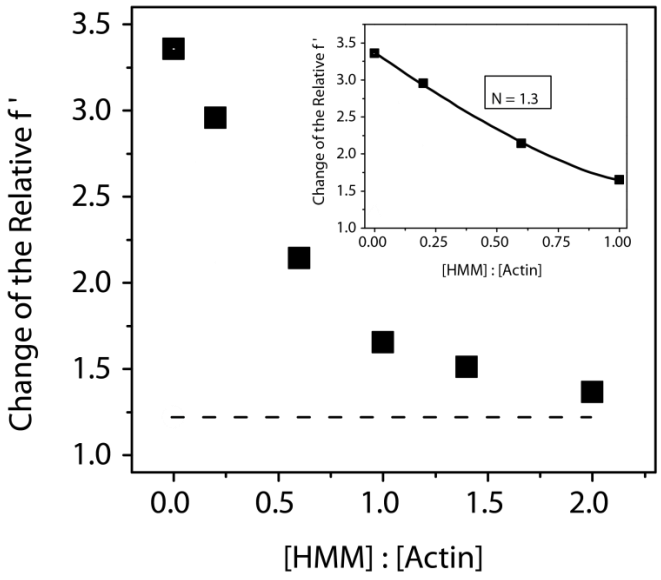

Figure 18 – The flexibility of actin filaments (the change of the relative *f '* between 6 and 34 °C) as a function of the HMM : actin concentration ratio. The experiments were carried out with 5 µM actin 500 nM mDia1-FH2 and HMM (as indicated). Filled squares were obtained with HMM. Dashed line indicates the value of the flexibility in the absence of formin and HMM. HMM concentrations are taken as heavy meromyosin head concentrations. Buffer conditions are as in *Fig. 17*. The inset shows the fits to the data using *Eq. 9* The length of the cooperative unit was found to be 1.3 ± 0.1 for HMM.

4.3 Study of the formin-induced flexibility reduction using anisotropy decay

The next method we used to confirm our previous FRET results was the measurement of anisotropy decay (*Fig. 19*). This method was used to describe the dynamic properties of actin many times before [144, 177, 178]. Our experiments were carried out with IAEDANS-labelled actin filaments. We applied 500 nM mDia1-FH2 concentration, which was shown to be enough to saturate the binding sites at the barbed ends of actin filaments [73, 179]. The evaluation of the data resulted in two rotational correlation times. The value of the shorter rotational correlation time was between 1-4 ns, and showed no formin, tropomyosin or heavy meromyosin concentration dependence. This shorter rotational correlation time – in our interpretation – can be related to the motion of the probe relative to the protein, which did not show significant formin-, tropomyosin- or HMM-induced changes. The value of the longer rotational correlation time showed formin-concentration dependence and its value was ~ 700-900 ns in the absence of formin which decreased

to ~ 225-250 ns in the presence of 500 nM mDia1-FH2 (*Fig. 20* and *23*). This observation is in agreement with our previous results [144, 145] and indicated that formin binding made the actin filaments more flexible.

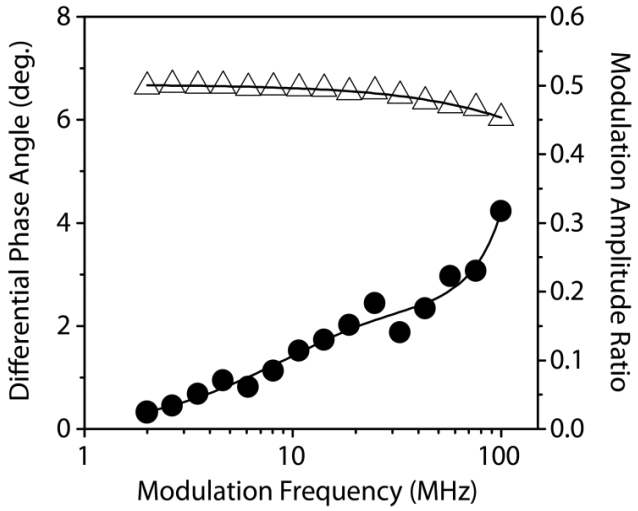

Figure 19 – Frequency-dependent phase (filled circles) and amplitude (empty triangles) data and a corresponding fit with double exponential function from anisotropy decay measurement.

4.3.1 The effect of tropomyosin measured by anisotropy decay

Anisotropy decay experiments were carried out using formin-bound actin filaments in the presence of tropomyosin at various concentrations (*Fig. 20*). The value of the longer rotational correlation time increased with increasing tropomyosin concentrations from 250 ns (the value in the absence of tropomyosin) to ~ 800 ns. In the case when the actin concentration was 30 µM the longer rotational correlation time reached its plateau at ~ 4 µM tropomyosin concentration (*Fig. 20A*) while at 20 µM actin concentration the breaking point appeared at ~ 3 µM tropomyosin (*Fig. 20B*). These tropomyosin concentrations which were giving the highest effect correlate well with the [tropomyosin] : [actin] = 1 : 7 binding stoichiometry, indicating that all the tropomyosin binding sites were occupied on the actin filaments at these states. The fact that the longer rotational correlation times of formin-bound actin filaments remained constant under saturating conditions indicated that the relatively

flexible formin-bound actin filaments were stabilized by the binding of tropomyosin, in agreement with our conclusion from the FRET results (*Fig. 17A*).

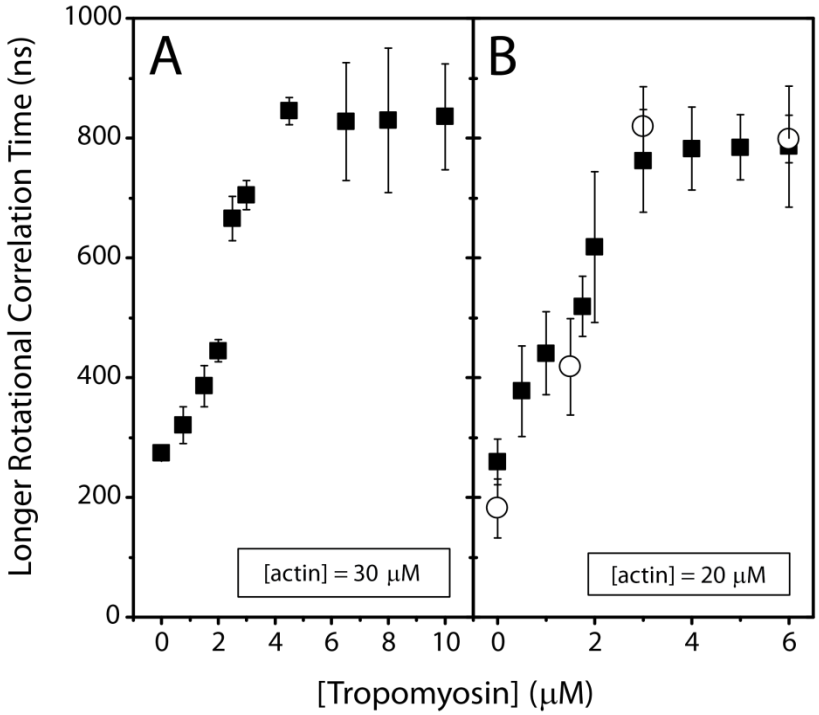

Figure 20 – Tropomyosin affects the anisotropy decay of formin-bound IAEDANS-actin filaments. The figure shows the tropomyosin concentration dependence of the longer rotational correlation times obtained for actin filaments. In panel **A** the actin concentration was 30 μM and the sample also contained 1.25 μM mDia1-FH2. Panel **B** shows the tropomyosin concentration dependence of the longer rotational correlation time measured with 20 μM actin and either 500 nM mDia1-FH2 (filled squares) or 500 nM mDia1-FH1FH2 (empty circles). The errors presented are standard errors from at least three independent experiments. Buffer conditions are as in *Fig. 17.*

In addition to FH2 the FH1 formin domain is also important in the biological function of formins [72]. In another set of anisotropy decay measurements we investigated whether the presence of the FH1 domain could modify the effect of the FH2 domain on the conformation of the actin filaments. These experiments were carried out at 20 μM actin and at a few mDia1-FH1FH2 concentrations. There was just a quite small difference between the longer rotational correlation times observed in the presence of mDia1-FH2 (~ 225-250 ns) and mDia1-FH1FH2 (~ 200 ns) in the absence of Tm, indicating that the binding of mDia1-FH1FH2 increased the flexibility of the actin filaments. When Tm was added to the mDia1-FH1FH2 bound actin filaments, the values of the longer rotational correlation time were increased and were identical

to those measured with mDia1-FH2 at the corresponding Tm concentrations (*Fig. 20B*). This observation suggested that the FH1 domain did not affect the effect of FH2 domain on the structure of the actin filaments.

4.3.1.1 Control experiments to check the affinity of tropomyosin for formin-nucleated actin filaments

Co-sedimentation experiments were carried out to exclude the possibility that the binding of formin weakens the affinity of tropomyosin for actin (*Fig. 21*). Samples were made containing tropomyosin (3 µM) and actin filaments (5 µM) in the absence or presence of formin (500 nM) and after they had been centrifuged (for 30 minutes at 386,000×*g* and at 20 °C) the pellets were analysed by SDS-PAGE. The amount of tropomyosin in the pellets was independent of the presence of formin, indicating that the mDia1-FH2 did not modify substantially the affinity of Tm for actin (*Fig. 21*). There is a formin band appeared in the pellets of tropomyosin-containing samples which showed that Tm did not displace the formins from actin. This state is in good agreement with the corresponding observations from Wawro and colleagues [135]. The gels also showed that there were not any contaminating proteins in these protein samples.

Figure 21 – Tropomyosin binds to the mDia1FH2 formin-bound actin filaments. SDS-PAGE gels of the pellets of actin, formin and tropomyosin samples from co-sedimentation assays. Lane **A** shows the molecular weight. Lane **B** shows the SDS-PAGE results obtained with 5 µM actin and 3 µM tropomyosin. Lane **C** shows the gel image for 5 µM actin, 0,5 µM formin and 3 µM tropomyosin. The experiments were carried out in 4 mM Tris-HCl (pH 7.3), 0.2 mM ATP, 0.1 mM $CaCl_2$, 0.5 mM DTT, 0.2 mM EGTA, 1 mM $MgCl_2$ and 50 mM KCl.

4.3.1.2 Salts that influence the effect of tropomyosin

Since previous studies showed that the effect of formins on actin filaments depends on ionic strength [144, 145], we tested the effect of potassium and magnesium on the interaction of Tm and mDia1-FH2-bound actin filaments by using fluorescence anisotropy decay. Our results on potassium salt dependence showed that the effect of Tm on actin filaments was independent of the KCl concentration between 10 mM and 30 mM KCl (*Fig. 22A*). In these experiments the concentration of $MgCl_2$ was 1 mM.

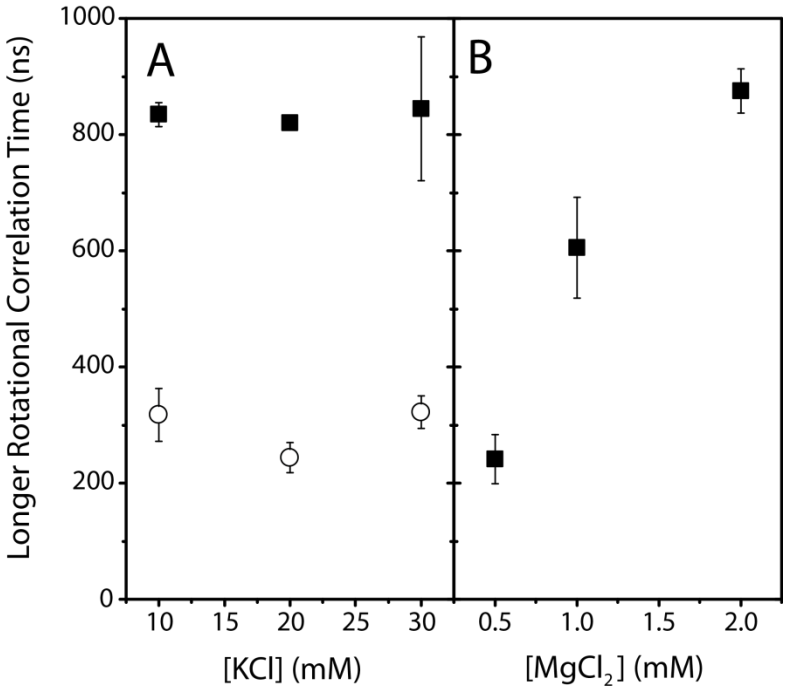

Figure 22 – The KCl and $MgCl_2$ dependence of the effect of tropomyosin on the flexibility of formin-bound actin filaments. Panel **A** shows the results obtained at fixed $MgCl_2$ concentration (1 mM) with 30 µM actin and 1.25 µM formin in either the absence (empty circles) or presence (filled squares) of tropomyosin (8 µM). The experiments were carried out at various KCl concentrations in 4 mM Tris-HCl (pH 7.3), 0.2 mM ATP, 0.1 mM $CaCl_2$, 0.5 mM DTT, 0.2 mM EGTA and 1 mM $MgCl_2$. In panel **B** results are presented from magnesium-dependent experiments at fixed KCl concentration (30 mM) with 30 µM actin, 1.25 µM formin and 4 µM tropomyosin. Other buffer conditions are as in *Fig. 17*.

The interaction between Tm and actin is magnesium dependent. The affinity of tropomyosin for actin, and the corresponding association and dissociation rates were magnesium concentration dependent [176]. The affinity is higher at higher $MgCl_2$ concentrations (K_D = 2.4 µM at 0.5 mM $MgCl_2$ and K_D = 0.5 µM at 2.5 mM $MgCl_2$).

These observations indicated that magnesium affects the interaction between Tm and actin. In these experiments tropomyosin and formin concentrations were 4 µM and 1.25 µM, respectively at 30 µM actin concentration. Fluorescence data showed that the longer rotational correlation time increased from ~ 250 ns at 0.5 mM $MgCl_2$ to ~ 850 ns at 2 mM $MgCl_2$ (*Fig. 22B*). This strong magnesium concentration dependence of the tropomyosin effect was in correlation with previous observations [176, 180] and indicated that magnesium is able to modify the tropomyosin induced stabilization effect on formin-bound actin filaments.

4.3.2 The effect of heavy meromyosin measured by anisotropy decay

We repeated the anisotropy decay experiments with formin-bound actin filaments in the presence of HMM at various concentrations (*Fig. 23*).

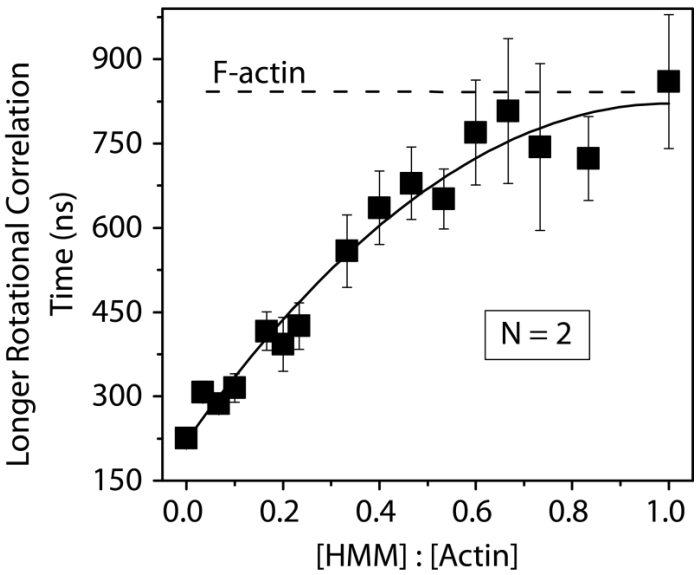

Figure 23 – Heavy meromyosin affects the anisotropy decay of formin-bound IAEDANS-actin filaments. Fitting the linear lattice model (shown as solid line, see: *Eq. 9*) gives N = 2.0 ± 0.3 actin protomers for the length of the cooperative unit. Dashed line indicates the value of the rotational correlation time measured in the absence of formin and HMM. The actin and mDia1-FH2 concentrations were 30 µM and 1.25 µM, respectively. The errors presented are standard errors from at least three independent experiments. Buffer conditions are as in *Fig. 17*.

The value of the longer rotational correlation time increased with increasing HMM concentrations from its value in the absence of HMM (225 ns) to ~ 850 ns *(Fig. 23)*. This indicates that formin-bound actin filaments were stiffer in the HMM-bound state. At greater HMM concentrations the conformation of the actin filaments became similar to that observed in the absence of formin and HMM. To estimate the number of actin protomers affected by the binding of one HMM head we applied the linear lattice model as described previously (*Eq. 9*, [150]). The length of the cooperative unit was found to be 2.0 ± 0.3 actin protomers (*Fig. 23*), indicating that the binding one HMM head could stabilize the conformation of two actin protomers.

4.4 Study of the formin-induced flexibility reduction using steady-state anisotropy

Steady-state fluorescence anisotropy measurements confirmed our previous results. The evaluation of the steady-state anisotropy data provides information on the flexibility of the experimental material in the cuvette, where a higher anisotropy value indicates a stiffer protein matrix. These experiments were also carried out with IAEDANS-labelled actin filaments.

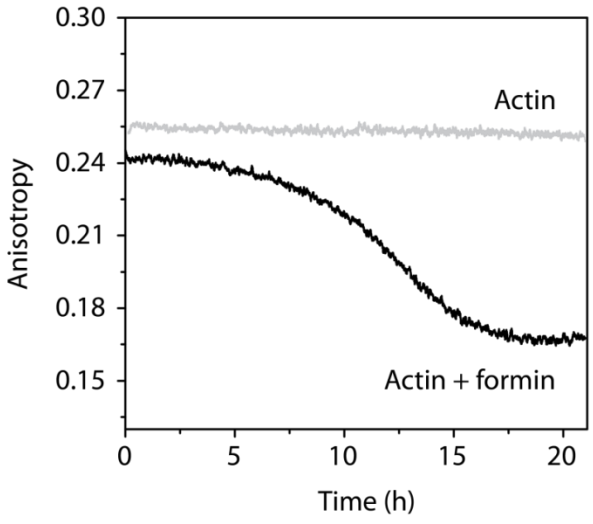

Figure 24 – Actin polymerized in the presence of formin at 20 mM KCl salt concentration. The recording of the data was started right after the mixing of the sample. The curves show the change in steady-state fluorescence anisotropy of IAEDANS-actin filaments (5 µM) measured in the absence (gray curve) or in the presence of 500 nM mDia1-FH2 (black curve).

Fluorescence anisotropy values of actin filaments alone were 0.25-0.26. After an overnight incubation with 500 nM mDia1-FH2 (that was the applied formin concentration in each sample), the value of anisotropy decreased to 0.14-0.17 depending on the time of incubation (*Fig. 24*). This observation is in correlation with our previous results obtained with other methods and confirms that the flexibility of the protein matrix increased upon binding of formin.

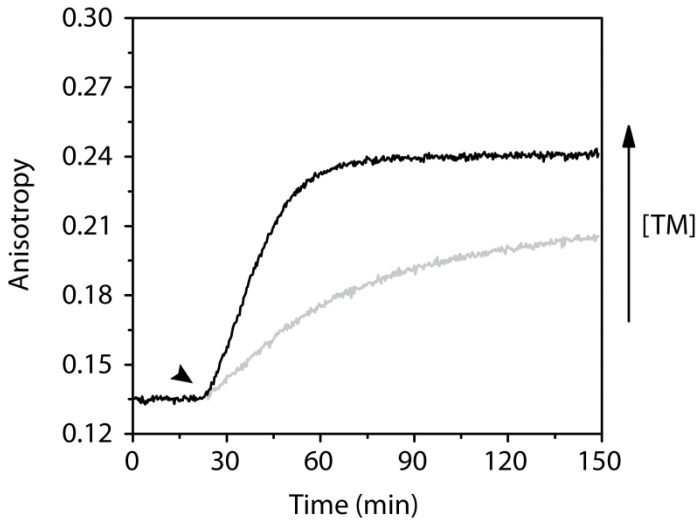

Figure 25 – The kinetics of the change in the steady-state fluorescence anisotropy of mDia1-FH2-nucleated (500 nM) IAEDANS-actin filaments (5 µM) measured in the presence of different amount of TM (1 µM (light gray curve), 5 µM (black curve)). Note that the steady-state anisotropy started to increase right after the addition of TM (indicated by an arrowhead) and plateaued within ~ 30 minutes at 20 mM KCl concentration.

When tropomyosin was added to the formin-bound, flexible actin filaments in different concentrations, the anisotropy started to increase slowly and a plateau appeared after ~ 30 minutes at anisotropy values ~ 0.25 (*Fig. 25*).

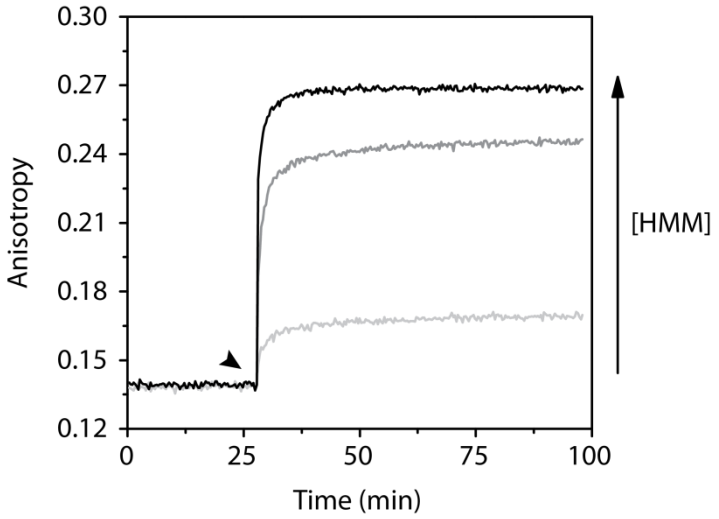

Figure 26 – The kinetics of the change in the steady-state anisotropy of mDia1-FH2-nucleated (500 nM) IAEDANS-actin filaments (5 µM) measured in the presence of different amount of HMM (1 µM (light gray curve), 5 µM (gray curve) and 10 µM (black curve)). Please note that the steady-state anisotropy started to increase right after the addition of HMM (indicated by an arrowhead) and plateaued within ~ 1 - 5 minutes at 25 mM KCl concentration.

When HMM was added to the sample after the overnight incubation with formin, the anisotropy increased rapidly (plateau was reached ~ 1 minute after the addition of HMM) to the values which are typical of actin alone (0.24-0.26 or above – depending on the concentration of the given HMM) (*Fig. 26*).

The steady-state anisotropy data were analysed by fitting single exponentials to the observed transients (*Eq. 3*). The amplitudes resolved in these fits gave the anisotropy increase (Δr) induced by the binding of either HMM or TM, and were plotted as a function of protein concentration in *Figure 27A* and *B*. Hyperbolic function was fitted (*Eq. 4*) to obtain the values of the maximum change (MAX) and half saturation protein concentrations ($K_{1/2}$) (*Fig. 27A* and *B*). For HMM the maximum anisotropy increase was 0.198 ± 0.01 and the half saturation was reached at 7.07 ± 1.3 µM HMM. This value is close to the applied actin concentration (5 µM). For TM we observed a maximum amplitude of 0.103 ± 0.0. This value is somewhat smaller than in the case of HMM suggesting that HMM is more effective in stabilizing the structure of the formin-nucleated actin filaments than TM. Half maximum was observed at 0.33 ± 0.13 µM TM. This half saturation concentration is about 10 fold less

than was observed for HMM, corresponding to the fact that one TM interacts with seven actin monomers in a filament [181].

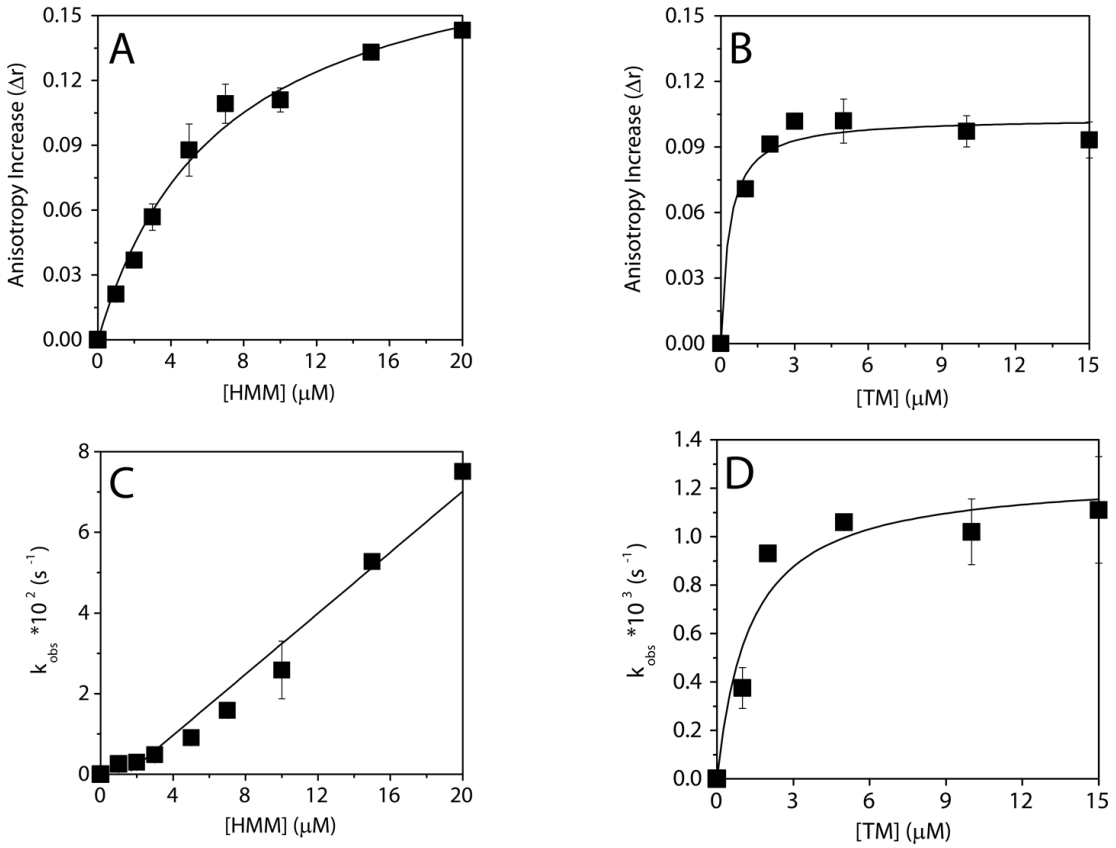

Figure 27 – The analysis of the effects of HMM and TM on the formin-induced conformational changes in actin filaments. ***(A, B)*** Anisotropy increase (*Δr*) as a function of HMM (***A***) or TM (***B***) concentration. Anisotropy increase was derived from the exponential fit (*Eq. 3*) of the data presented on *Fig. 25* and *26*. Note that a higher increase in the steady-state anisotropy from the low value of ~ 0.14 (characteristic for mDia1-FH2-nucleated actin filaments), indicates a greater stabilization of the conformational dynamics of mDia1-FH2-nucleated actin filaments. The data were analyzed by hyperbolic fits (*Eq. 4*) (dashed lines). The maximum values (*MAX*) were 0.198 ± 0.01 and 0.103 ± 0.00 for HMM and TM, respectively. The half saturation concentrations ($K_{1/2}$) were determined to be 7.074 ± 1.39 μM and 0.33 ± 0.13 μM for HMM and TM, respectively. (***C, D***) The observed rate constants (k_{obs}) as a function of HMM (***C***) or TM (***D***) concentration. The values of k_{obs} were derived from the exponential fit (*Eq. 3*) of the data presented on *Fig. 25* and *26*. The stabilizing effect of HMM on mDia1-FH2-nucleated actin filaments was rapid and the observed rate constant increased linearly with increasing amount of HMM. The stabilizing effect of TM on formin-nucleated actin filaments was much slower than that of HMM, and followed a hyperbolic tendency with increasing TM concentration. The errors presented on this figure are standard errors from at least two independent experiments.

We also analysed the HMM and TM concentration dependence of the rate constants (k_{obs}) derived from the exponential fits (*Fig. 27C* and *D*). In the case of HMM the k_{obs} values followed a quasi-linear tendency with increasing amount of HMM and did not reach a plateau up to about 0.1 s^{-1} (*Fig. 27C*). This kinetic behaviour indicates that HMM binding to the formin-nucleated actin filaments occurs as an apparent single-step reaction. Interestingly, the slope of the fit (reflecting an apparent on-rate constant of 0.004 $\mu M^{-1}s^{-1}$) was much lower than that determined earlier from pyrene-actin fluorescence intensity changes upon skeletal muscle myosin S1 binding to actin filaments in the absence of formin. The latter value was in the order of 10 $\mu M^{-1}s^{-1}$ [182-184]. However, it should be stressed that the large difference from the present result may at least in part originate from the different types of signal reporting different structural changes during the actin binding process. For TM the k_{obs} vs. TM concentration curve showed a saturating tendency (*Fig. 27D*). This kinetic behaviour is indicative of a two-step reaction in which the added TM binds to the actin filament, and then a first order conformational transition occurs in the complex. Interestingly, the maximal observed rate constant, reflecting the first-order transition, was much lower than the rate constants observed in the case of HMM (*Fig. 27C*). These findings imply that, despite the apparently similar reversal of formin-induced conformational changes by HMM and TM, the kinetic mechanism of this process is markedly different in the case of these two actin-binding proteins.

5 Conclusions

These new results emphasize the importance of the intramolecular conformational changes induced by formins in the structure of actin filaments. The mDia1 formin changed the conformation of the protein matrix in the subdomain 1 of the actin protomers. It seems reasonable to assume that these flexible actin filaments serve well-defined biological aims, which are manifested under special intracellular conditions. However, one would also assume that other conditions require actin networks with mechanically stabile, more rigid filaments. We therefore expected that actin-binding proteins could reverse the formin-induced structural changes by binding to filaments. Tropomyosin and heavy meromyosin were tested whether they can stabilize the conformation of the actin filaments. The results presented in my thesis indicate that both of these abundant actin-binding proteins were able to reverse the formin induced conformational changes. The experimental data proved that the molecular mechanisms exerted by the effect of tropomyosin and heavy meromyosin play a central role in the molecular mechanisms regulating the conformational dynamics of actin filaments. We speculate that the greater flexibility of the filaments observed in the presence of formins may result from the rapid and special way of formin-assisted polymerization. For the proper functioning of actin filaments, the conformational state with a more rigid structure is probably preferable, and thus there are molecular repair mechanisms which reverse the formin-induced flexibility changes. These mechanisms are based on the binding of actin-binding proteins. With the results presented here there are now two abundant binding partners of actin identified – TM and HMM – that can play such regulatory roles. Their common property is that the binding of both of these proteins cooperatively affects the structure of the actin filaments along a stretch of several protomers.

My present results serve new perspectives towards further investigations to identify other actin-binding proteins which play a regulatory role in the fine-tuning of actin conformation. These proteins should be studied in complex systems to reveal how the different effects of actin-binding proteins on the conformational properties of

actin are superimposed (synergistically or antagonistically) to establish the overall conformational dynamics and the biological function of cellular actin structures. This way we can examine the different contender processes during the organization and realignment of the cytoskeleton.

6 List of abbreviations

ADF: actin depolymerizing factor

ADP: adenosine-5'-diphosphate

Arp2/3: Actin-related protein 2/3

ATP: adenosine-5'-triphosphate

CapZ: actin filament barbed end capping protein (CP) from the Z-disc of muscle

EDTA: ethylenediaminetetraacetic acid

EGTA: ethylene glycol tetraacetic acid

For3p: a *Schizosaccharomyces pombe* formin

Fus1p: yeast cell fusion protein 1

g: gravitational acceleration

GDP: guanosine-5'-diphosphate

GTP: guanosine-5'-triphosphate

hDia: human homologue of Drosophila Diaphanous

LB: Lysogeny broth (Luria broth, Lennox broth or Luria-Bertani medium)

P_i: inorganic phosphate

Rac: subfamily of the Rho family of GTPases

RhoA: Ras homolog gene family, member A

Scar: suppressor of cyclic AMP receptor (a WASP related protein)

SDS-PAGE: sodium dodecyl sulfate polyacrylamide gel electrophoresis

Tris: (hydroxymethyl)aminomethane

WASP: Wiskott–Aldrich Syndrome Protein

WH2: Wiskott-Aldrich syndrome homology region 2

7 References

1. Prasain, N. and T. Stevens, *The actin cytoskeleton in endothelial cell phenotypes.* Microvasc Res, 2009. **77**(1): p. 53-63.
2. Oelz, D., C. Schmeiser, and J.V. Small, *Modeling of the actin-cytoskeleton in symmetric lamellipodial fragments.* Cell Adh Migr, 2008. **2**(2): p. 117-26.
3. Dominguez, R., *Actin filament nucleation and elongation factors--structure-function relationships.* Crit Rev Biochem Mol Biol, 2009. **44**(6): p. 351-66.
4. Evangelista, M., S. Zigmond, and C. Boone, *Formins: signaling effectors for assembly and polarization of actin filaments.* J Cell Sci, 2003. **116**(Pt 13): p. 2603-11.
5. Higgs, H.N. and T.D. Pollard, *Regulation of actin filament network formation through ARP2/3 complex: activation by a diverse array of proteins.* Annu Rev Biochem, 2001. **70**: p. 649-76.
6. Schaefer, A.W., et al., *Coordination of actin filament and microtubule dynamics during neurite outgrowth.* Dev Cell, 2008. **15**(1): p. 146-62.
7. Uribe, R. and D. Jay, *A review of actin binding proteins: new perspectives.* Mol Biol Rep, 2009. **36**(1): p. 121-5.
8. Semenova, I., et al., *Actin dynamics is essential for myosin-based transport of membrane organelles.* Curr Biol, 2008. **18**(20): p. 1581-6.
9. Lacayo, C.I., et al., *Emergence of large-scale cell morphology and movement from local actin filament growth dynamics.* PLoS Biol, 2007. **5**(9): p. e233.
10. Bubb, M.R., et al., *Polylysine induces an antiparallel actin dimer that nucleates filament assembly: crystal structure at 3.5-A resolution.* J Biol Chem, 2002. **277**(23): p. 20999-1006.
11. Sept, D. and J.A. McCammon, *Thermodynamics and kinetics of actin filament nucleation.* Biophys J, 2001. **81**(2): p. 667-74.
12. Carballido-Lopez, R., *The bacterial actin-like cytoskeleton.* Microbiol Mol Biol Rev, 2006. **70**(4): p. 888-909.
13. Esue, O., et al., *The assembly of MreB, a prokaryotic homolog of actin.* J Biol Chem, 2005. **280**(4): p. 2628-35.
14. Thanbichler, M. and L. Shapiro, *Getting organized--how bacterial cells move proteins and DNA.* Nat Rev Microbiol, 2008. **6**(1): p. 28-40.
15. Shaevitz, J.W. and Z. Gitai, *The structure and function of bacterial actin homologs.* Cold Spring Harb Perspect Biol, 2010. **2**(9): p. a000364.
16. Huxley, H.E., ed. *The structure and function of muscle*. ed. G.H. Bourne. Vol. 1. 1972, Academic Press, New York. 301-387.
17. Straub, F.B., *Actin.* Studies from the Institute of Medical Chemistry, Szeged, 1942. **2**(3): p. 15.
18. Bárány, M. and K. Bárány. *Actin*. 2002;
Available from: http://www.uic.edu/classes/phyb/phyb516/actinu3.htm.
19. Feuer, G., et al., *Studies on the composition and polymerisation of actin.* Hung. Acta Physiol., 1948. **1**: p. 150-163.
20. Straub, F.B. and G. Feuer, *Adenosine triphosphate, the functional group of actin.* Kiserl Orvostud, 1950. **2**(2): p. 141-51.
21. Holmes, K.C., and Kabsch, W. , *Muscle proteins: actin.* Current Opinion in Structural Biology, 1991. **1**(2): p. 270-280.
22. Wagner, C.R., A.P. Mahowald, and K.G. Miller, *One of the two cytoplasmic actin isoforms in Drosophila is essential.* Proc Natl Acad Sci U S A, 2002. **99**(12): p. 8037-42.
23. Cooper, G.M., *The Cell, A Molecular Approach*. 2nd ed. 2000: Sinauer Associates, Inc.

24. wordiQ. *Sarcomere*. 2010;
Available from: http://www.wordiq.com/definition/Sarcomere.
25. www.miami.edu. 2002;
Available from: http://www.bio.miami.edu/~cmallery/150/neuro/sf43x15a.jpg.
26. Pollard, T.D. and J.A. Cooper, *Actin, a central player in cell shape and movement.* Science, 2009. **326**(5957): p. 1208-12.
27. Chhabra, E.S. and H.N. Higgs, *The many faces of actin: matching assembly factors with cellular structures.* Nat Cell Biol, 2007. **9**(10): p. 1110-21.
28. Pollard, T.D., *Regulation of actin filament assembly by Arp2/3 complex and formins.* Annu Rev Biophys Biomol Struct, 2007. **36**: p. 451-77.
29. Chesarone, M.A., A.G. DuPage, and B.L. Goode, *Unleashing formins to remodel the actin and microtubule cytoskeletons.* Nat Rev Mol Cell Biol, 2010. **11**(1): p. 62-74.
30. Caldwell, J.E., et al., *Effects of CapZ, an actin capping protein of muscle, on the polymerization of actin.* Biochemistry, 1989. **28**(21): p. 8506-14.
31. Zigmond, S.H., *Formin-induced nucleation of actin filaments.* Curr Opin Cell Biol, 2004. **16**(1): p. 99-105.
32. Theriot, J.A., *Accelerating on a treadmill: ADF/cofilin promotes rapid actin filament turnover in the dynamic cytoskeleton.* J Cell Biol, 1997. **136**(6): p. 1165-8.
33. Goley, E.D., et al., *An actin-filament-binding interface on the Arp2/3 complex is critical for nucleation and branch stability.* Proc Natl Acad Sci USA, 2010. **107**(18): p. 8159-64.
34. Mullins, R.D., W.F. Stafford, and T.D. Pollard, *Structure, subunit topology, and actin-binding activity of the Arp2/3 complex from Acanthamoeba.* J Cell Biol, 1997. **136**(2): p. 331-43.
35. Quinlan, M.E., et al., *Drosophila Spire is an actin nucleation factor.* Nature, 2005. **433**(7024): p. 382-8.
36. Chereau, D., et al., *Leiomodin is an actin filament nucleator in muscle cells.* Science, 2008. **320**(5873): p. 239-43.
37. Ahuja, R., et al., *Cordon-bleu is an actin nucleation factor and controls neuronal morphology.* Cell, 2007. **131**(2): p. 337-50.
38. Goley, E.D. and M.D. Welch, *The ARP2/3 complex: an actin nucleator comes of age.* Nat Rev Mol Cell Biol, 2006. **7**(10): p. 713-26.
39. Winckler, B. and D.A. Schafer, *Cordon-bleu: a new taste in actin nucleation.* Cell, 2007. **131**(2): p. 236-8.
40. Conley, C.A., et al., *Leiomodins: larger members of the tropomodulin (Tmod) gene family.* Genomics, 2001. **73**(2): p. 127-39.
41. Shimada, A., et al., *The core FH2 domain of diaphanous-related formins is an elongated actin binding protein that inhibits polymerization.* Mol. Cell, 2004. **13**(4): p. 511-22.
42. Trumpp, A., et al., *The chicken limb deformity gene encodes nuclear proteins expressed in specific cell types during morphogenesis.* Genes Dev, 1992. **6**(1): p. 14-28.
43. Tanaka, K., *Formin family proteins in cytoskeletal control.* Biochem Biophys Res Commun, 2000. **267**(2): p. 479-81.
44. Chalkia, D., et al., *Origins and evolution of the formin multigene family that is involved in the formation of actin filaments.* Mol Biol Evol, 2008. **25**(12): p. 2717-33.
45. Grunt, M., V. Zarsky, and F. Cvrckova, *Roots of angiosperm formins: the evolutionary history of plant FH2 domain-containing proteins.* BMC Evol Biol, 2008. **8**: p. 115.
46. Higgs, H.N., *Formin proteins: a domain-based approach.* Trends Biochem Sci, 2005. **30**(6): p. 342-53.
47. Favaro, P.M., et al., *High expression of FMNL1 protein in T non-Hodgkin's lymphomas.* Leuk Res, 2006. **30**(6): p. 735-8.

48. Lizarraga, F., et al., *Diaphanous-related formins are required for invadopodia formation and invasion of breast tumor cells.* Cancer Res, 2009. **69**(7): p. 2792-800.
49. Zhu, X.L., L. Liang, and Y.Q. Ding, *Overexpression of FMNL2 is closely related to metastasis of colorectal cancer.* Int J Colorectal Dis, 2008. **23**(11): p. 1041-7.
50. Evangelista, M., et al., *Bni1p, a yeast formin linking cdc42p and the actin cytoskeleton during polarized morphogenesis.* Science, 1997. **276**(5309): p. 118-22.
51. Longtine, M.S., et al., *The septins: roles in cytokinesis and other processes.* Curr Opin Cell Biol, 1996. **8**(1): p. 106-19.
52. Harris, E.S., et al., *Mechanistic differences in actin bundling activity of two mammalian formins, FRL1 and mDia2.* J Biol Chem, 2006. **281**(20): p. 14383-92.
53. Michelot, A., et al., *The formin homology 1 domain modulates the actin nucleation and bundling activity of Arabidopsis FORMIN1.* Plant Cell, 2005. **17**(8): p. 2296-313.
54. Moseley, J.B. and B.L. Goode, *Differential activities and regulation of Saccharomyces cerevisiae formin proteins Bni1 and Bnr1 by Bud6.* J Biol Chem, 2005. **280**(30): p. 28023-33.
55. Vaillant, D.C., et al., *Interaction of the N- and C-terminal autoregulatory domains of FRL2 does not inhibit FRL2 activity.* J Biol Chem, 2008. **283**(48): p. 33750-62.
56. Chhabra, E.S. and H.N. Higgs, *INF2 Is a WASP homology 2 motif-containing formin that severs actin filaments and accelerates both polymerization and depolymerization.* J Biol Chem, 2006. **281**(36): p. 26754-67.
57. Harris, E.S., F. Li, and H.N. Higgs, *The mouse formin, FRLalpha, slows actin filament barbed end elongation, competes with capping protein, accelerates polymerization from monomers, and severs filaments.* J Biol Chem, 2004. **279**(19): p. 20076-87.
58. Yi, K., et al., *Cloning and functional characterization of a formin-like protein (AtFH8) from Arabidopsis.* Plant Physiol, 2005. **138**(2): p. 1071-82.
59. Dong, Y., D. Pruyne, and A. Bretscher, *Formin-dependent actin assembly is regulated by distinct modes of Rho signaling in yeast.* J Cell Biol, 2003. **161**(6): p. 1081-92.
60. Castrillon, D.H. and S.A. Wasserman, *Diaphanous is required for cytokinesis in Drosophila and shares domains of similarity with the products of the limb deformity gene.* Development, 1994. **120**(12): p. 3367-77.
61. Kovar, D.R., et al., *The fission yeast cytokinesis formin Cdc12p is a barbed end actin filament capping protein gated by profilin.* J Cell Biol, 2003. **161**(5): p. 875-87.
62. Li, F. and H.N. Higgs, *The mouse Formin mDia1 is a potent actin nucleation factor regulated by autoinhibition.* Curr Biol, 2003. **13**(15): p. 1335-40.
63. Pruyne, D., et al., *Role of formins in actin assembly: nucleation and barbed-end association.* Science, 2002. **297**(5581): p. 612-5.
64. Sagot, I., et al., *An actin nucleation mechanism mediated by Bni1 and profilin.* Nat Cell Biol, 2002. **4**(8): p. 626-31.
65. Bartolini, F., et al., *The formin mDia2 stabilizes microtubules independently of its actin nucleation activity.* J Cell Biol, 2008. **181**(3): p. 523-36.
66. Lewkowicz, E., et al., *The microtubule-binding protein CLIP-170 coordinates mDia1 and actin reorganization during CR3-mediated phagocytosis.* J Cell Biol, 2008. **183**(7): p. 1287-98.
67. Wen, Y., et al., *EB1 and APC bind to mDia to stabilize microtubules downstream of Rho and promote cell migration.* Nat Cell Biol, 2004. **6**(9): p. 820-30.
68. Zigmond, S.H., et al., *Formin leaky cap allows elongation in the presence of tight capping proteins.* Curr Biol, 2003. **13**(20): p. 1820-3.
69. Kovar, D.R. and T.D. Pollard, *Insertional assembly of actin filament barbed ends in association with formins produces piconewton forces.* Proc Natl Acad Sci U S A, 2004. **101**(41): p. 14725-30.
70. Watanabe, N. and C. Higashida, *Formins: processive cappers of growing actin filaments.* Exp Cell Res, 2004. **301**(1): p. 16-22.

71. Vidali, L., et al., *Rapid formin-mediated actin-filament elongation is essential for polarized plant cell growth.* Proc Natl Acad Sci U S A, 2009. **106**(32): p. 13341-6.
72. Goode, B.L. and M.J. Eck, *Mechanism and function of formins in the control of actin assembly.* Annu Rev Biochem, 2007. **76**: p. 593-627.
73. Romero, S., et al., *Formin is a processive motor that requires profilin to accelerate actin assembly and associated ATP hydrolysis.* Cell, 2004. **119**(3): p. 419-29.
74. Petersen, J., et al., *FH3, a domain found in formins, targets the fission yeast formin Fus1 to the projection tip during conjugation.* J Cell Biol, 1998. **141**(5): p. 1217-28.
75. Wallar, B.J. and A.S. Alberts, *The formins: active scaffolds that remodel the cytoskeleton.* Trends Cell Biol, 2003. **13**(8): p. 435-46.
76. Fujiwara, T., et al., *Bni1p regulates microtubule-dependent nuclear migration through the actin cytoskeleton in Saccharomyces cerevisiae.* Mol Cell Biol, 1999. **19**(12): p. 8016-27.
77. Giansanti, M.G., et al., *Cooperative interactions between the central spindle and the contractile ring during Drosophila cytokinesis.* Genes Dev, 1998. **12**(3): p. 396-410.
78. Goode, B.L., D.G. Drubin, and G. Barnes, *Functional cooperation between the microtubule and actin cytoskeletons.* Curr Opin Cell Biol, 2000. **12**(1): p. 63-71.
79. Waterman-Storer, C.M. and E. Salmon, *Positive feedback interactions between microtubule and actin dynamics during cell motility.* Curr Opin Cell Biol, 1999. **11**(1): p. 61-7.
80. Palazzo, A.F., et al., *mDia mediates Rho-regulated formation and orientation of stable microtubules.* Nat Cell Biol, 2001. **3**(8): p. 723-9.
81. Kato, T., et al., *Localization of a mammalian homolog of diaphanous, mDia1, to the mitotic spindle in HeLa cells.* J Cell Sci, 2001. **114**(Pt 4): p. 775-84.
82. Wasserman, S., *FH proteins as cytoskeletal organizers.* Trends Cell Biol, 1998. **8**(3): p. 111-5.
83. Imamura, H., et al., *Bni1p and Bnr1p: downstream targets of the Rho family small G-proteins which interact with profilin and regulate actin cytoskeleton in Saccharomyces cerevisiae.* EMBO J, 1997. **16**(10): p. 2745-55.
84. Robinson, N.G., et al., *Rho3 of Saccharomyces cerevisiae, which regulates the actin cytoskeleton and exocytosis, is a GTPase which interacts with Myo2 and Exo70.* Mol Cell Biol, 1999. **19**(5): p. 3580-7.
85. Watanabe, N., et al., *p140mDia, a mammalian homolog of Drosophila diaphanous, is a target protein for Rho small GTPase and is a ligand for profilin.* EMBO J, 1997. **16**(11): p. 3044-56.
86. Gasteier, J.E., et al., *Activation of the Rac-binding partner FHOD1 induces actin stress fibers via a ROCK-dependent mechanism.* J Biol Chem, 2003. **278**(40): p. 38902-12.
87. Koka, S., et al., *The formin-homology-domain-containing protein FHOD1 enhances cell migration.* J Cell Sci, 2003. **116**(Pt 9): p. 1745-55.
88. Watanabe, N., et al., *Cooperation between mDia1 and ROCK in Rho-induced actin reorganization.* Nat Cell Biol, 1999. **1**(3): p. 136-43.
89. Heasman, S.J. and A.J. Ridley, *Mammalian Rho GTPases: new insights into their functions from in vivo studies.* Nat Rev Mol Cell Biol, 2008. **9**(9): p. 690-701.
90. Etienne-Manneville, S. and A. Hall, *Rho GTPases in cell biology.* Nature, 2002. **420**(6916): p. 629-35.
91. Hill, C.S., J. Wynne, and R. Treisman, *The Rho family GTPases RhoA, Rac1, and CDC42Hs regulate transcriptional activation by SRF.* Cell, 1995. **81**(7): p. 1159-70.
92. Alberts, A.S., *Identification of a carboxyl-terminal diaphanous-related formin homology protein autoregulatory domain.* J Biol Chem, 2001. **276**(4): p. 2824-30.
93. Gasman, S., Y. Kalaidzidis, and M. Zerial, *RhoD regulates endosome dynamics through Diaphanous-related Formin and Src tyrosine kinase.* Nat Cell Biol, 2003. **5**(3): p. 195-204.

94. Witke, W., *The role of profilin complexes in cell motility and other cellular processes.* Trends Cell Biol, 2004. **14**(8): p. 461-9.
95. Chang, F., D. Drubin, and P. Nurse, *cdc12p, a protein required for cytokinesis in fission yeast, is a component of the cell division ring and interacts with profilin.* J Cell Biol, 1997. **137**(1): p. 169-82.
96. Severson, A.F., D.L. Baillie, and B. Bowerman, *A Formin Homology protein and a profilin are required for cytokinesis and Arp2/3-independent assembly of cortical microfilaments in C. elegans.* Curr Biol, 2002. **12**(24): p. 2066-75.
97. Pring, M., et al., *Mechanism of formin-induced nucleation of actin filaments.* Biochemistry, 2003. **42**(2): p. 486-96.
98. Feierbach, B. and F. Chang, *Roles of the fission yeast formin for3p in cell polarity, actin cable formation and symmetric cell division.* Curr Biol, 2001. **11**(21): p. 1656-65.
99. Murai, K. and R. Treisman, *Interaction of serum response factor (SRF) with the Elk-1 B box inhibits RhoA-actin signaling to SRF and potentiates transcriptional activation by Elk-1.* Mol Cell Biol, 2002. **22**(20): p. 7083-92.
100. Sotiropoulos, A., et al., *Signal-regulated activation of serum response factor is mediated by changes in actin dynamics.* Cell, 1999. **98**(2): p. 159-69.
101. Yasui, B., F. Fuchs, and F.N. Briggs, *The role of the sulfhydryl groups of tropomyosin and troponin in the calcium control of actomyosin contractility.* J Biol Chem, 1968. **243**(4): p. 735-42.
102. Mizuno, H., et al., *Tropomyosin as a regulator of the sliding movement of actin filaments.* Biosystems, 2007. **90**(2): p. 449-55.
103. Gunning, P., G. O'Neill, and E. Hardeman, *Tropomyosin-based regulation of the actin cytoskeleton in time and space.* Physiol Rev, 2008. **88**(1): p. 1-35.
104. Bach, C.T., et al., *Tropomyosin isoform modulation of focal adhesion structure and cell migration.* Cell Adh Migr, 2010. **4**(2): p. 226-34.
105. Dufour, C., R.P. Weinberger, and P. Gunning, *Tropomyosin isoform diversity and neuronal morphogenesis.* Immunol Cell Biol, 1998. **76**(5): p. 424-9.
106. Bailey, K., *Tropomyosin: a new asymmetric protein component of the muscle fibril.* Biochem J, 1948. **43**(2): p. 271-9.
107. Brown, J.H. and C. Cohen, *Regulation of muscle contraction by tropomyosin and troponin: how structure illuminates function.* Adv Protein Chem, 2005. **71**: p. 121-59.
108. Hitchcock-DeGregori, S.E., *Tropomyosin: function follows structure.* Adv Exp Med Biol, 2008. **644**: p. 60-72.
109. Lehman, W. and R. Craig, *Tropomyosin and the steric mechanism of muscle regulation.* Adv Exp Med Biol, 2008. **644**: p. 95-109.
110. Perry, S.V., *Vertebrate tropomyosin: distribution, properties and function.* J Muscle Res Cell Motil, 2001. **22**(1): p. 5-49.
111. Greenfield, N.J., et al., *The structure of the N-terminus of striated muscle alpha-tropomyosin in a chimeric peptide: nuclear magnetic resonance structure and circular dichroism studies.* Biochemistry, 1998. **37**(21): p. 7834-43.
112. Muthuchamy, M., et al., *Molecular and physiological effects of overexpressing striated muscle beta-tropomyosin in the adult murine heart.* J Biol Chem, 1995. **270**(51): p. 30593-603.
113. Tobacman, L.S., *Thin filament-mediated regulation of cardiac contraction.* Annu Rev Physiol, 1996. **58**: p. 447-81.
114. Gunning, P.W., et al., *Tropomyosin isoforms: divining rods for actin cytoskeleton function.* Trends Cell Biol, 2005. **15**(6): p. 333-41.
115. Gunning, P., et al., *Differential control of tropomyosin mRNA levels during myogenesis suggests the existence of an isoform competition-autoregulatory compensation control mechanism.* Dev Biol, 1990. **138**(2): p. 443-53.

116. Lees-Miller, J.P. and D.M. Helfman, *The molecular basis for tropomyosin isoform diversity.* Bioessays, 1991. **13**(9): p. 429-37.
117. Lees-Miller, J.P., L.O. Goodwin, and D.M. Helfman, *Three novel brain tropomyosin isoforms are expressed from the rat alpha-tropomyosin gene through the use of alternative promoters and alternative RNA processing.* Mol Cell Biol, 1990. **10**(4): p. 1729-42.
118. Stamm, S., et al., *Brain-specific tropomyosins TMBr-1 and TMBr-3 have distinct patterns of expression during development and in adult brain.* Proc Natl Acad Sci U S A, 1993. **90**(21): p. 9857-61.
119. Schevzov, G., et al., *Tissue-specific tropomyosin isoform composition.* J Histochem Cytochem, 2005. **53**(5): p. 557-70.
120. Cooper, H.L., et al., *Suppression of tropomyosin synthesis, a common biochemical feature of oncogenesis by structurally diverse retroviral oncogenes.* Mol Cell Biol, 1985. **5**(5): p. 972-83.
121. Franzen, B., et al., *Expression of tropomyosin isoforms in benign and malignant human breast lesions.* Br J Cancer, 1996. **73**(7): p. 909-13.
122. Hendricks, M. and H. Weintraub, *Tropomyosin is decreased in transformed cells.* Proc Natl Acad Sci U S A, 1981. **78**(9): p. 5633-7.
123. Leavitt, J., et al., *Expression of transfected mutant beta-actin genes: transitions toward the stable tumorigenic state.* Mol Cell Biol, 1987. **7**(7): p. 2467-76.
124. Matsumura, F., et al., *Differential expression of tropomyosin forms in the microfilaments isolated from normal and transformed rat cultured cells.* J Biol Chem, 1983. **258**(22): p. 13954-64.
125. Wang, F.L., et al., *Two differentially expressed genes in normal human prostate tissue and in carcinoma.* Cancer Res, 1996. **56**(16): p. 3634-7.
126. Hughes, J.A., et al., *High-molecular-weight tropomyosins localize to the contractile rings of dividing CNS cells but are absent from malignant pediatric and adult CNS tumors.* Glia, 2003. **42**(1): p. 25-35.
127. Bryce, N.S., et al., *Specification of actin filament function and molecular composition by tropomyosin isoforms.* Mol Biol Cell, 2003. **14**(3): p. 1002-16.
128. Bretscher, A., *Polarized growth and organelle segregation in yeast: the tracks, motors, and receptors.* J Cell Biol, 2003. **160**(6): p. 811-6.
129. Anyanful, A., et al., *The third and fourth tropomyosin isoforms of Caenorhabditis elegans are expressed in the pharynx and intestines and are essential for development and morphology.* J Mol Biol, 2001. **313**(3): p. 525-37.
130. Kreuz, A.J., A. Simcox, and D. Maughan, *Alterations in flight muscle ultrastructure and function in Drosophila tropomyosin mutants.* J Cell Biol, 1996. **135**(3): p. 673-87.
131. Tansey, T., et al., *Small differences in Drosophila tropomyosin expression have significant effects on muscle function.* Mol Cell Biol, 1991. **11**(12): p. 6337-42.
132. Tetzlaff, M.T., H. Jackle, and M.J. Pankratz, *Lack of Drosophila cytoskeletal tropomyosin affects head morphogenesis and the accumulation of oskar mRNA required for germ cell formation.* EMBO J, 1996. **15**(6): p. 1247-54.
133. Blanchard, E.M., et al., *Targeted ablation of the murine alpha-tropomyosin gene.* Circ Res, 1997. **81**(6): p. 1005-10.
134. Rethinasamy, P., et al., *Molecular and physiological effects of alpha-tropomyosin ablation in the mouse.* Circ Res, 1998. **82**(1): p. 116-23.
135. Wawro, B., et al., *Tropomyosin regulates elongation by formin at the fast-growing end of the actin filament.* Biochemistry, 2007. **46**(27): p. 8146-55.
136. Evangelista, M., et al., *Formins direct Arp2/3-independent actin filament assembly to polarize cell growth in yeast.* Nat Cell Biol, 2002. **4**(3): p. 260-9.
137. Pruyne, D. and A. Bretscher, *Polarization of cell growth in yeast. I. Establishment and maintenance of polarity states.* J Cell Sci, 2000. **113 (Pt 3)**: p. 365-75.

138. Pruyne, D. and A. Bretscher, *Polarization of cell growth in yeast.* J Cell Sci, 2000. **113 (Pt 4)**: p. 571-85.
139. Wu, J.Q., et al., *Spatial and temporal pathway for assembly and constriction of the contractile ring in fission yeast cytokinesis.* Dev Cell, 2003. **5**(5): p. 723-34.
140. Sellers, J.R., ed. *Protein Profile: Myosins. 2nd Ed.* 1999, Oxford Univ. Press, Oxford.
141. Conti, M.A. and R.S. Adelstein, *Nonmuscle myosin II moves in new directions.* J Cell Sci, 2008. **121**(Pt 1): p. 11-8.
142. Chen, L.F., et al., *Molecular modeling of averaged rigor crossbridges from tomograms of insect flight muscle.* J Struct Biol, 2002. **138**(1-2): p. 92-104.
143. Cytoskeleton. *Heavy meromyosin protein*. 1993-2011; Available from: http://www.cytoskeleton.com/products/motor/mh01.html.
144. Bugyi, B., et al., *Formins regulate actin filament flexibility through long range allosteric interactions.* J. Biol. Chem., 2006. **281**(16): p. 10727-36.
145. Papp, G., et al., *Conformational changes in actin filaments induced by formin binding to the barbed end.* Biophys J, 2006. **91**(7): p. 2564-72.
146. Ujfalusi, Z., et al., *Effect of tropomyosin on formin-bound actin filaments.* Biophys. J., 2009. **96**(1): p. 162-68.
147. Kovar, D.R., V. Sirotkin, and M. Lord, *Three's company: the fission yeast actin cytoskeleton.* Trends Cell Biol, 2010.
148. Tojkander, S., et al., *A Molecular Pathway for Myosin II Recruitment to Stress Fibers.* Curr Biol, 2011. **21**(7): p. 539-50.
149. Orlova, A. and E.H. Egelman, *Cooperative rigor binding of myosin to actin is a function of F-actin structure.* J. Mol. Biol., 1997. **265**(5): p. 469-74.
150. Prochniewicz, E. and D.D. Thomas, *Perturbations of functional interactions with myosin induce long-range allosteric and cooperative structural changes in actin.* Biochemistry, 1997. **36**(42): p. 12845-53.
151. Prochniewicz, E. and D.D. Thomas, *Site-specific mutations in the myosin binding sites of actin affect structural transitions that control myosin binding.* Biochemistry, 2001. **40**(46): p. 13933-40.
152. Prochniewicz, E., T.F. Walseth, and D.D. Thomas, *Structural dynamics of actin during active interaction with myosin: different effects of weakly and strongly bound myosin heads.* Biochemistry, 2004. **43**(33): p. 10642-52.
153. Prochniewicz, E., et al., *Myosin Isoform Determines the Conformational Dynamics and Cooperativity of Actin Filaments in the Strongly Bound Actomyosin Complex.* J. Mol. Biol., 2010. **26**(396): p. 501-509.
154. Spudich, J.A. and S. Watt, *The regulation of rabbit skeletal muscle contraction. I. Biochemical studies of the interaction of the tropomyosin-troponin complex with actin and the proteolytic fragments of myosin.* J. Biol. Chem., 1971. **246**(15): p. 4866-71.
155. Houk, T.W., Jr. and K. Ue, *The measurement of actin concentration in solution: a comparison of methods.* Anal. Biochem., 1974. **62**(1): p. 66-74.
156. Elzinga, M., et al., *Complete amino-acid sequence of actin of rabbit skeletal muscle.* Proc. Natl. Acad. Sci. U. S. A., 1973. **70**(9): p. 2687-91.
157. Eisenberg, E. and W.W. Kielley, *Troponin-tropomyosin complex. Column chromatographic separation and activity of the three, active troponin components with and without tropomyosin present.* J. Biol. Chem., 1974. **249**(15): p. 4742-8.
158. Smillie, L.B., *Preparation and identification of alpha- and beta-tropomyosins.* Methods Enzymol., 1982. **85 Pt B**: p. 234-41.
159. Margossian, S.S. and S. Lowey, *Preparation of myosin and its subfragments from rabbit skeletal muscle.* Methods Enzymol., 1982. **85 Pt B**: p. 55-71.
160. Miki, M., C.G. dos Remedios, and J.A. Barden, *Spatial relationship between the nucleotide-binding site, Lys-61 and Cys-374 in actin and a conformational change induced by myosin subfragment-1 binding.* Eur. J. Biochem., 1987. **168**(2): p. 339-45.

161. Hudson, E.N. and G. Weber, *Synthesis and characterization of two fluorescent sulfhydryl reagents.* Biochemistry, 1973. **12**(21): p. 4154-61.
162. Hild, G., M. Nyitrai, and B. Somogyi, *Intermonomer flexibility of Ca- and Mg-actin filaments at different pH values.* Eur. J. Biochem., 2002. **269**(3): p. 842-9.
163. Miki, M., *Resonance energy transfer between points in a reconstituted skeletal muscle thin filament. A conformational change of the thin filament in response to a change in Ca2+ concentration.* Eur. J. Biochem., 1990. **187**(1): p. 155-62.
164. Ujfalusi, Z., et al., *The effects of formins on the conformation of subdomain 1 in actin filaments.* J Photochem Photobiol B, 2010. **98**(1): p. 7-11.
165. Jameson, D.M., J.C. Croney, and P.D. Moens, *Fluorescence: basic concepts, practical aspects, and some anecdotes.* Methods Enzymol, 2003. **360**: p. 1-43.
166. Somogyi, B., et al., *Forster-type energy transfer as a probe for changes in local fluctuations of the protein matrix.* Biochemistry, 1984. **23**(15): p. 3403-11.
167. Somogyi, B., et al., *Protein flexibility as revealed by fluorescence resonance energy transfer: an extension of the method for systems with multiple labels.* J. Photochem. Photobiol. B, 2000. **59**(1-3): p. 26-32.
168. Lakowicz, J.R., *Principles of Fluorescence Spectroscopy*. 3rd ed. 2006: Springer. 960.
169. Uversky, V.N., *Methods in Protein Structure and Stability Analysis: Conformational Stability, Size, Shape and Surface of Protein Molecules*, ed. V. Uversky and E. Permyakov. 2007: Nova Publishers. 404.
170. Lakowicz, J.R., *Principles of fluorescence spectroscopy*. 1983, New York: Plenum press. 75-81.
171. Belford, G.G., R.L. Belford, and G. Weber, *Dynamics of fluorescence polarization in macromolecules.* Proc. Natl. Acad. Sci. U. S. A., 1972. **69**(6): p. 1392-3.
172. Orlova, A. and E.H. Egelman, *Structural dynamics of F-actin: I. Changes in the C terminus.* J Mol Biol, 1995. **245**(5): p. 582-97.
173. Orlova, A., E. Prochniewicz, and E.H. Egelman, *Structural dynamics of F-actin: II. Cooperativity in structural transitions.* J Mol Biol, 1995. **245**(5): p. 598-607.
174. Romero, S., et al., *How ATP hydrolysis controls filament assembly from profilin-actin: implication for formin processivity.* J. Biol. Chem., 2007. **282**(11): p. 8435-45.
175. Kovacs, M., et al., *Load-dependent mechanism of nonmuscle myosin 2.* Proc. Natl. Acad. Sci. U. S. A., 2007. **104**(24): p. 9994-9.
176. Wegner, A., *Equilibrium of the actin-tropomyosin interaction.* J. Mol. Biol., 1979. **131**(4): p. 839-53.
177. Miki, M., P. Wahl, and J.C. Auchet, *Fluorescence anisotropy of labeled F-actin: influence of divalent cations on the interaction between F-actin and myosin heads.* Biochemistry, 1982. **21**(15): p. 3661-5.
178. Miki, M., P. Wahl, and J.C. Auchet, *Fluorescence anisotropy of labelled F-actin. Influence of Ca2+ on the flexibility of F-actin.* Biophys. Chem., 1982. **16**(2): p. 165-72.
179. Li, F. and H.N. Higgs, *The mouse Formin mDia1 is a potent actin nucleation factor regulated by autoinhibition.* Curr. Biol., 2003. **13**(15): p. 1335-40.
180. Fowler, V.M. and V. Bennett, *Erythrocyte membrane tropomyosin. Purification and properties.* J. Biol. Chem., 1984. **259**(9): p. 5978-89.
181. Yang, Y.Z., E.D. Korn, and E. Eisenberg, *Cooperative binding of tropomyosin to muscle and Acanthamoeba actin.* J Biol Chem, 1979. **254**(15): p. 7137-40.
182. Coates, J.H., A.H. Criddle, and M.A. Geeves, *Pressure-relaxation studies of pyrene-labelled actin and myosin subfragment 1 from rabbit skeletal muscle. Evidence for two states of acto-subfragment 1.* Biochem J, 1985. **232**(2): p. 351-6.
183. Takacs, B., et al., *Myosin cleft closure determines the energetics of the actomyosin interaction.* FASEB J, 2011. **25**(1): p. 111-21.
184. Taylor, E.W., *Kinetic studies on the association and dissociation of myosin subfragment 1 and actin.* J Biol Chem, 1991. **266**(1): p. 294-302.

8 Publications

8.1 Publications related to the Thesis

1. **The Effects of Formins on the Conformation of Subdomain 1 in Actin Filaments**. **Ujfalusi, Z.**, Barkó, Sz., Hild, G., Nyitrai, M. *Journal of Photochemistry and Photobiology B-Biology* **98:(1)** pp. 7-11. (2010)

   IF: 1.871; Citations: 2

2. **The effect of tropomyosin on formin-bound actin filaments**. **Ujfalusi, Z.**, Vig, A., Hild, G., Nyitrai, M. *Biophysical Journal* **96:(1)** pp. 162-168. (2009)

   IF: 4.390; Citations: 2

8.2 Conference presentations related to the Thesis

1. **Aktin-kötő fehérjék hatása az aktin filamentumok flexibilitására. Ujfalusi, Z.**, Vig, A., Nagy, N., Kovács, M., Hild, G. and Nyitrai, M., – oral presentation at the XXIIIrd Congress of the Hungarian Biophysical Society (23-26 August, 2009, Pécs).

2. **The effect of actin binding proteins on the flexibility of formin-bound actin filaments**. **Ujfalusi Z.**, Vig, A., Nagy, N., Kovács, M., Hild, G. and Nyitrai, M. – oral presentation at the Symposium for Graduate Students in Biology (12-13 November, 2009, Pécs).

3. **The effect tropomyosin and heavy meromyosin on the flexibility of formin-bound actin filaments. Ujfalusi, Z.**, Nyitrai, M. and Hild, G. – oral presentation at the Intracellular Fluorescence Spectroscopy Satellite Conference of the 8th European Biophysics Congress (20-22 August, 2011, Pécs).

8.3 Other publications

1. **Conformational Changes in Actin Filaments Induced by Formin Binding to the Barbed End**. Papp, G., Bugyi, B., **Ujfalusi, Z.**, Barkó, Sz., Hild, G., Somogyi, B., Nyitrai, M. *Biophysical Journal* **91:(7)** pp. 2564-2572. (2006)

   IF: 4.757; Citations: 6

2. **The effect of pyrene labelling on the thermal stability of actin filaments**. Halasi, Sz., Papp, G., Bugyi, B., Barkó, Sz., Orbán, J., **Ujfalusi, Z.**, Visegrády, B. *Thermochimica Acta* **(445)** pp. 185-189. (2006)

   IF: 1.417; Citations: 2

3. **The effect of pH on the thermal stability of alpha-actin isoforms**. Papp, G., Bugyi, B., **Ujfalusi, Z.**, Halasi, Sz., Orbán, J. *Thermochimica Acta* **(82)** pp. 281-285. (2005)

   IF: 1.230; Citations: 4

Cumulative impact factor: 13.665 Sum of independent citations: 16